

The following had been originally translated from:

Paulke S., Köster D., Hass R., Bader V., Menzel S., Gubalke A.: „Thermische Simulationen einer Volkswagen e-Golf-Fahrzeugkabine unter Einbezug von thermischen Menschmodellen“, SIMVEC, 17.Kongress, VDI-Berichten 2224, S.555-588 (2014)

## **Thermal Simulations of a Volkswagen e-Golf Cabin Incorporating Human Thermal Comfort Models**

Dr. Stefan Paulke, Dr. Daniel Köster, Dr. Regina Hass (P+Z Engineering GmbH), Dr. Viktor Bader, Dr. Stephan Menzel, Andreas Gubalke (Volkswagen AG)

### **Abstract**

As part of the publicly funded BMBF<sup>1</sup> project, E-Komfort involved generating a highly detailed finite element<sup>2</sup> model for simulating the climate control system of the passenger compartment of a Volkswagen e-Golf. This article will demonstrate how an FE crash model was used as a basis for developing a cabin model for interior climate control systems. Shown here are the results from simulations in an environmental chamber under winter and summer load conditions relevant to vehicle design and range. This work also involved testing and calibrating special lamp models (for simulating sunlight in environmental chambers), and then using these models in the simulation. In this paper we will describe an initial validation study demonstrating that, in addition to simulating the average temperature of the cabin air - an important aspect of thermal comfort - models also do a very good job of mapping local air temperatures.

We will then illustrate how we extrapolated and calibrated a simplified cabin model (known as a rapid or generator model) from a highly detailed e-Golf simulation model. Doing so allowed us to reduce computing time from several days to a few seconds without compromising the quality of the simulated average temperature of the cabin air.

Using THESEUS-FE simulations, we were able to demonstrate that employing zonal climate control concepts can massively reduce the amount of energy that the climate control system consumes. Energy can also be conserved through the use of infrared emitters, which were simulated using suitable models and assessed in terms of their impact on local thermal

---

<sup>1</sup> BMBF = Bundesministerium für Bildung und Forschung, the German Federal Ministry of Education and Research

<sup>2</sup> The term “finite element” will be represented by the abbreviation “FE” in the following.

comfort values. Under winter load conditions, e-vehicle range is significantly limited by the amount of energy consumed by the climate control system. As such, heating or cooling passengers only where needed and/or only to a comfortable temperature makes more sense than heating/cooling the entire passenger compartment. Against this backdrop, our simulation also incorporated a thermophysiological model and used the concept of equivalent temperature as a basis for assessing local thermal comfort.

The final portion of this paper provides a discussion of motivation and strategies for coupled cabin simulations - in this case coupling THESEUS-FE and OpenFOAM - as well as the corresponding validation work.

### 1. Setting up a detailed thermal vehicle model for cabin simulation

The early phase of E-Komfort involved developing an FE model of the overall vehicle that would be as true to detail as possible. The starting point for this work was a meshed simulation model used for testing crash/side-impact protection systems. Used for evaluating structural mechanics, this model simulates, among other parameters, all of the bonding technology used, i.e., all weld points and adhesives. When developing the thermal cabin model, we incorporated the bonding technology in full so that we could map any thermal bridges in detail.

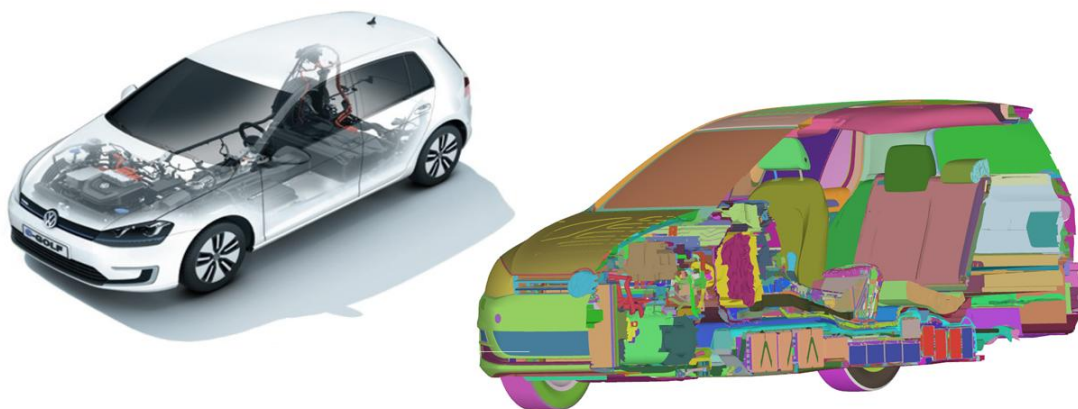


Figure 1: VW e-Golf: reality and the THESEUS-FE simulation model (cross-section)

This stage of model development also took the following into consideration:

Due to their low load-bearing capacity, certain components (the roof, plastic panels, seats, carpet, insulating elements, windows, etc.) are either not included in the crash model or are only represented in a simplified way. Such components are, however, significant considerations in sophisticated climate control systems and, as such, were remeshed. Volume meshes, typically tetrahedral elements, were used for simulating the thermally

conductive properties of components with irregular thicknesses or with complex layered structures (such as the dashboard, insulating elements, seats, etc.) (see figure 2).

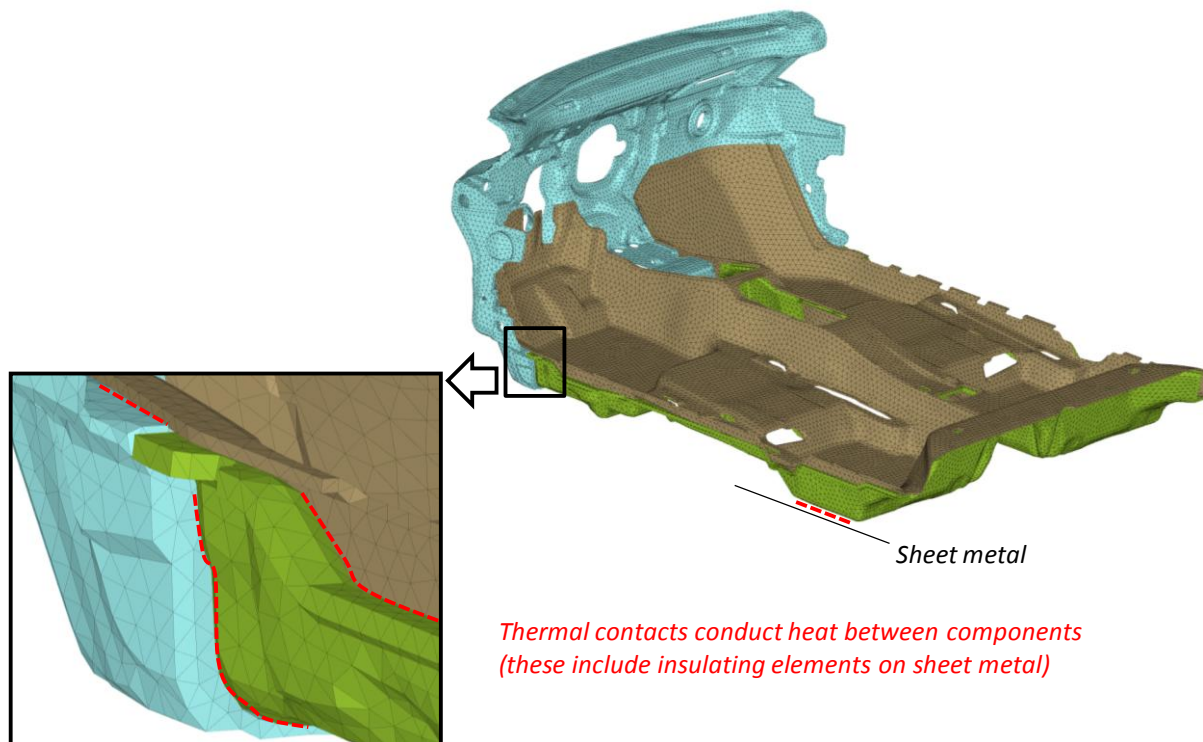


Figure 2: Carpet and insulating elements in the bulkheads and floor (FE model with tetrahedral meshing)

For components with large contact areas (as shown in figure 2), thermal contacts were used that generate a thermally conductive bond via an automatic assignment process.

Working closely with Volkswagen Group research, we developed an extensive database of thermal conductivity material parameters. The challenge here lay in assigning the correct values for thermal conductivity ( $\lambda$  in  $\text{W/m}^2\text{K}$ ) and specific heat ( $c_p$  in  $\text{J/kgK}$ ) for the materials used in the e-Golf. While gathering physically correct material parameters was particularly time-consuming for glass, plastic and foams, this task was absolutely imperative, as virtually all of the surfaces that come into contact with the cabin air are made of these materials. Heat transfer between the cabin air and the surfaces that it contacts is an especially important consideration when studying the energy balance and power that a climate control system needs. When developing the simulation model, we took great care to save the data source for each material card in addition to names and physical properties.

Correctly mapping the physical phenomenon of radiation (especially at the windows) meant having to store the corresponding properties - transmission, reflection, absorption, etc. - as material properties dependent on angle and wavelength. When factoring in solar radiation, we used wavelength-dependent transmittance in order to record the spectrum of sunlight correctly ( $\lambda=300 - 2500$  nm), and determined weighted transmittance as described in DIN EN 410 (see figure 3). Angle  $\varphi$  describes the angle between the solar radiation and the normal to the window.

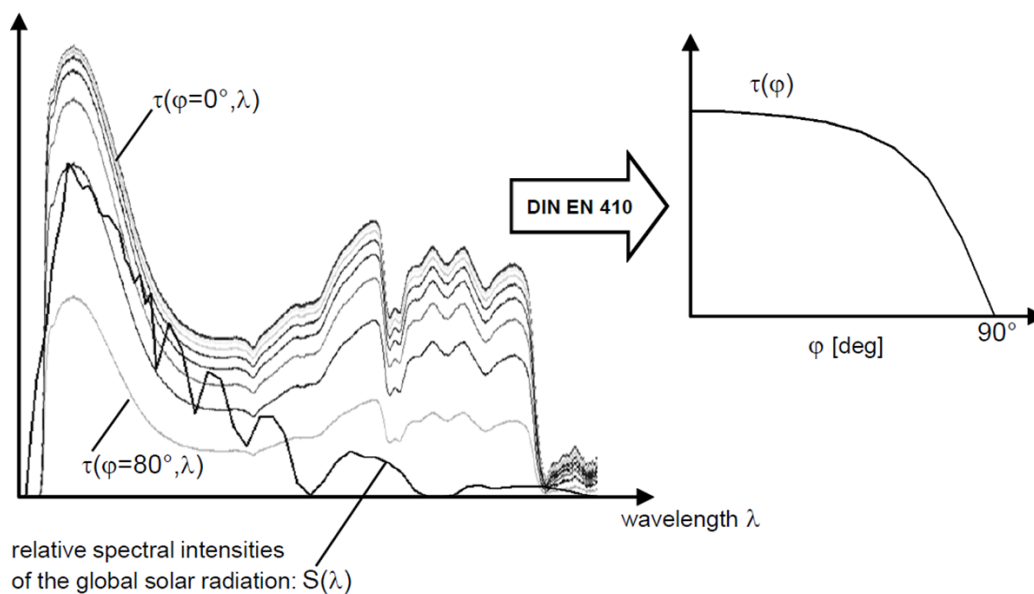


Figure 3: Sample curves showing transmittance [15] as a function of wavelength and angle

Standard THESEUS-FE software methods (ray tracing and accelerated data structures known as *k-d trees*) were used for calculating view factors ( $FE \leftrightarrow FE$  and  $sun \rightarrow FE$ ) on surface elements.<sup>3</sup>

In order to create a simplified model of convective heat transfer between the air and the components of the vehicle, cabin air was divided into what are referred to as “air zones” (figure 4). The first step here was simply to map the average temperature and humidity in each of these zones, with the model accounting for mass flows between these air zones (such as those between the footwell and the cabin air above). The enthalpy flow that the climate control system introduces into the cabin was calculated as a function of volume flow,

<sup>3</sup> Some 2 million shell elements in the e-Golf FE model at 2 surfaces each translates to 4 million surface elements.

humidity and temperature of the air inflow<sup>4</sup>, using the corresponding characteristic values for the e-Golf. Volume flow and air input temperature are shown in figure 5 as qualitative examples of typical summer load conditions.

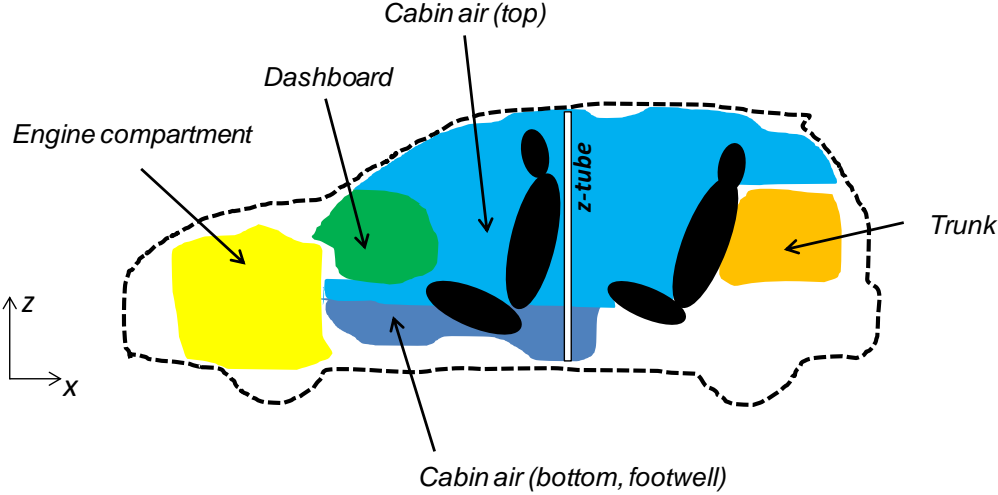


Figure 4: Air zones in the simulation model

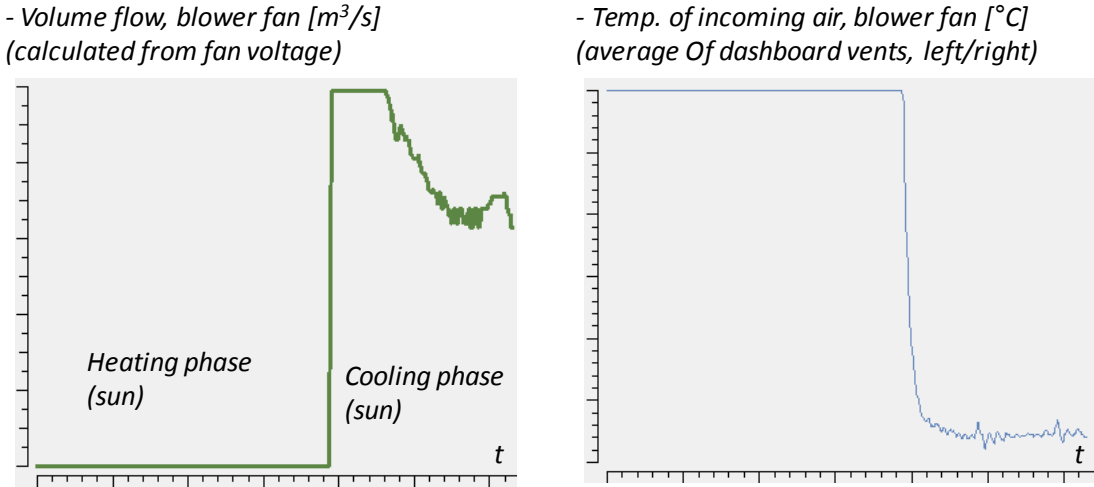


Figure 5: Typical climate control parameters (summer load)

In order to map convective heat transfer in small air cavities<sup>5</sup>, we used a method that involved automatically detecting cavities and assigning constant air temperatures to those cavities during the simulation. These constant temperatures were derived from the average of adjacent element surfaces. The coefficient of convective heat transfer in the cavities was

<sup>4</sup> See [12].

<sup>5</sup> This refers to all air cavities not indicated by a color in figure 4, such as those in the roof or door.

estimated here as  $h \approx 2 \text{ W/m}^2\text{K}$ .<sup>6</sup> When convective heat transfer in cavities was low (stagnant air), the importance of heat transfer due to thermal radiation increased (FE $\leftrightarrow$ FE). Under ideal circumstances—between two infinitely extended plates—this heat transfer (in  $\text{W/m}^2$ ) can be calculated as follows:

$$\dot{q}_{\text{rad}}^n = \frac{\sigma}{\frac{1}{\varepsilon^{n-1}} + \frac{1}{\varepsilon^{n+1}} - 1} \left[ (\bar{T}^{n-1})^4 - (\bar{T}^{n+1})^4 \right]$$

where  $\sigma$  is the Stefan-Boltzmann constant and  $\varepsilon$  is the coefficient of emission, and  $\bar{T}$  indicates the temperature in degrees Kelvin. The view factor<sup>7</sup> was equal to 1 for infinitely extended surfaces.

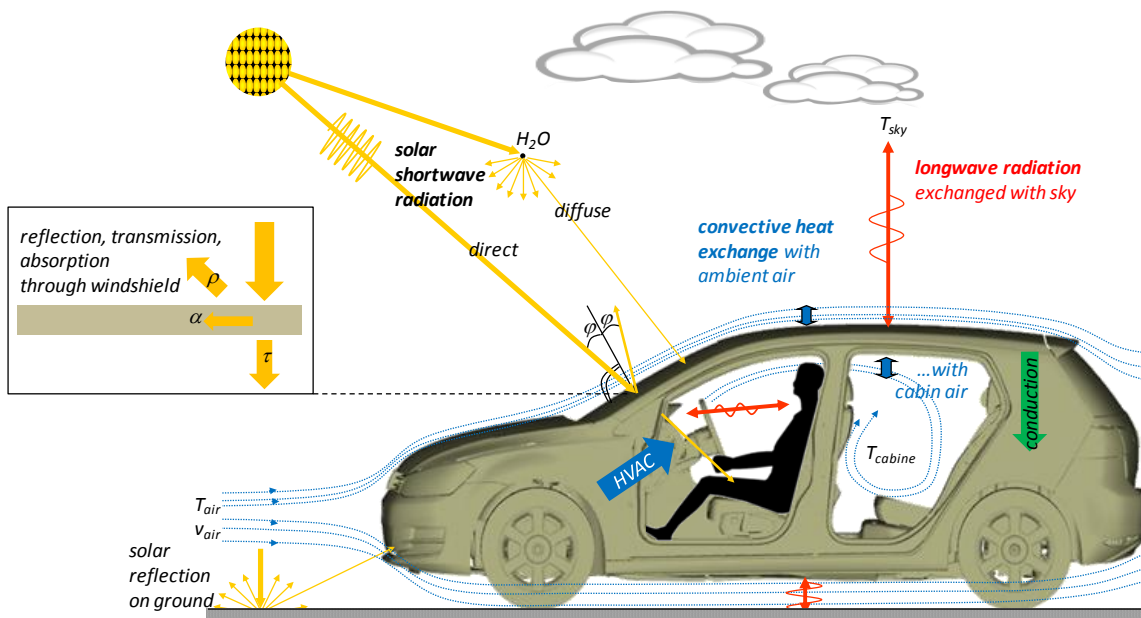


Figure 6: Thermal transfer phenomena [3] under true summer load conditions.

The vehicle was preconditioned at an ambient temperature of  $35^\circ\text{C}$  in the Volkswagen environmental chamber under typical summer load conditions, after which artificial suns (54

<sup>6</sup>This estimate is based on methods found in the literature for analyzing free convection in cavities [13]. Using the (typical) summer and winter load conditions investigated here, we were able to demonstrate that a value of  $h \approx 2 \text{ W/m}^2\text{K}$  is a good approximation.

<sup>7</sup> As part of a realistic simulation (THESEUS-FE, etc.), view factors ( $<1$ ) were calculated in advance between surfaces at different temperatures and then entered into what is known as a view factor matrix.

lamps) were switched on to heat up the vehicle and the cabin slowly. The intensity of the solar radiation typically reached values of up to  $1000 \text{ W/m}^2$  on the vehicle's exterior. During the warming phase, the cabin air heats up continuously, whereby input heat is largely the result of solar radiation falling on the windows and being absorbed by vehicle components (such as the dashboard). The heat absorbed is then transferred to the air via convection. Components heated by the sun also emit heat via thermal radiation resulting from the temperature difference between components, a phenomenon also referred to as longwave radiation ( $\lambda > 2500 \text{ nm}$ ). The sun emits primarily shortwave radiation ( $300 - 2500 \text{ nm}$ ). While shortwave solar radiation is transmitted through the windows, the greenhouse effect keeps longwave thermal radiation inside the cabin, as the windows are essentially non-transparent at those wavelengths.

Figure 6 shows all of the major heat transfer phenomena under real summer load conditions (air flows and convective heat transfer are shown in blue; longwave heat transfer via radiation is shown in red; shortwave solar radiation is shown in yellow). HVAC (heating ventilation air conditioning) is the term used to describe a climate control system that uses its own cooling power ( $\dot{H}$ ) to cancel out heat introduced from outside ( $\dot{Q}$ ):

$$\dot{Q} + \dot{H} = 0 \text{ (operating with recirculated air)}$$

The amount of cooling power needed is larger when operating with outside air, as the air drawn in from outside is generally warmer than the cabin air during the summer. This is why modern, energy-saving climate control concepts avoid the exclusive use of outside air and instead blend outside air with recirculated air.

Heat coming in from outside ( $\dot{Q}$ ) largely enters the cabin via the windows. Suitable insulating elements (see figure 2) and air cavities provide considerable thermal insulation for other heat transfer routes in the e-Golf. The impact of the high-gloss paint is negligible. The simulation results on the roof reveal that the highly insulating, layered structure of the roof (metal – insulation – air – roof lining) allows very little heat to penetrate, regardless of the paint or external absorptivity, even when the sun's rays are directed down at a  $90^\circ$  angle.

## **2. Lamp models for the environmental chamber**

We implemented a detailed model of the environmental chamber with 54 lamps so that the simulation model would reflect reality as closely possible. The tremendous distance between the sun and Earth makes the actual sun a near perfect source of parallel light rays, whereas the distances between the lamps and the e-Golf in the environmental chamber are quite short by comparison (see figure 7). This led to the assumption that the rays reaching the

outer shell of the e-Golf model could be highly inhomogeneous. In this case, “inhomogeneous” is defined as follows:

- The solar radiation reaching the vehicle is highly dependent on the z-axis.
- The solar radiation reaching the vehicle varies considerably in the x-y plane (along the roof, for example).
- Because of the angled components of the rays, considerably more solar radiation will enter the cabin than is the case with the actual sun (which emits parallel light rays).

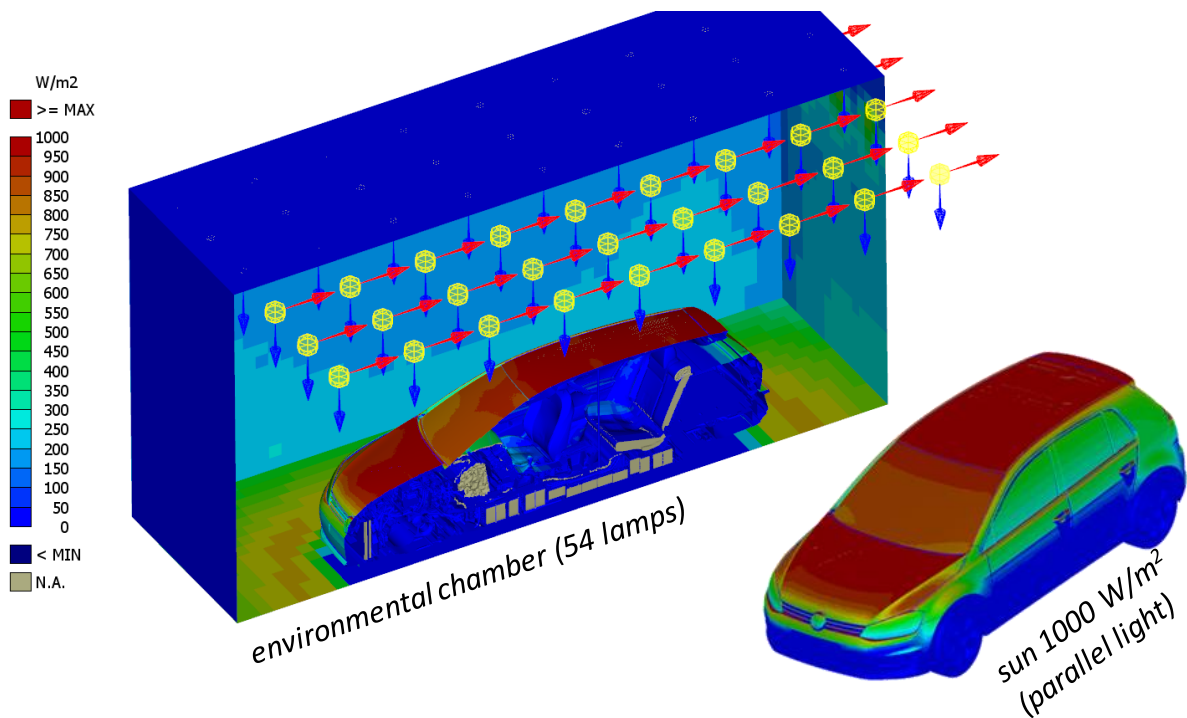


Figure 7: Simulated solar radiation in the environmental chamber (with 54 lamps) and actual solar radiation

In order to validate the simulation, a single lamp was analyzed by measuring intensity as a function of distance  $r$  and of angles  $\psi$  and  $\varphi$  (see figure 8). This was then used for generating a lamp model for THESEUS-FE having a point source as shown in figure 8. Figure 7 shows solar radiation coverage in the simulation using all 54 lamps in the environmental chamber. The small vehicle in figure 7 (below right) shows actual solar radiation of  $1000 \text{ W/m}^2$  for comparison. The two models are highly similar: taken together, the 54 lamps generate roughly  $1000 \text{ W/m}^2$  along the roof.

Despite how well the two models agreed, the simulation demonstrated that lamps - due to the non-vertical light rays they produce - transferred somewhat more heat into the cabin than was the case for the actual sun. Surprisingly, the intensity of the radiation was found to be virtually independent of the z-coordinate, despite the short distance between the lamps and the vehicle.

We then studied the lamps to determine whether the spectrum of radiated wavelengths is comparable to that of the sun. Agreement was sufficiently good that no changes to the model were required. A temperature of  $T_{\text{sky}} = 50^\circ\text{C}$  was used in the simulation for studying the longwave radiation exchange between the roof of the environmental chamber and the surface of the vehicle.

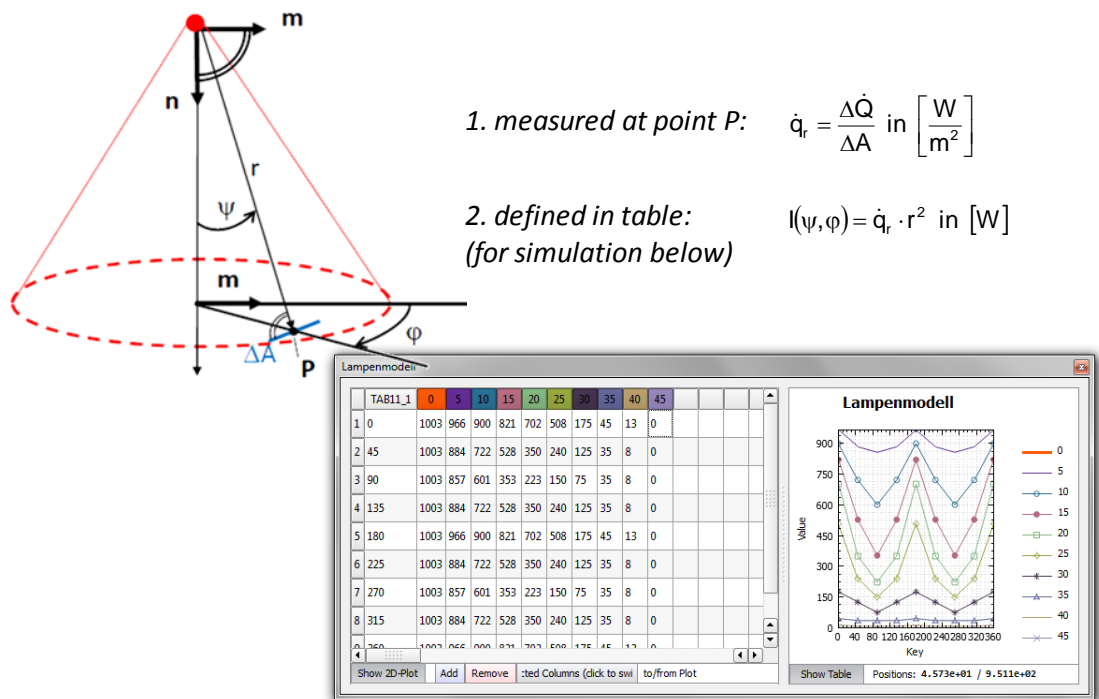


Figure 8: Definition of a solar point source in the THESEUS-FE software [12]

### 3. Initial validation work and climate control variations for the vehicle interior

Over the course of validating the thermal simulation model, we were able to demonstrate that the overall mass of the model agreed with that of the actual e-Golf. The simulation model was validated using real climate load conditions.

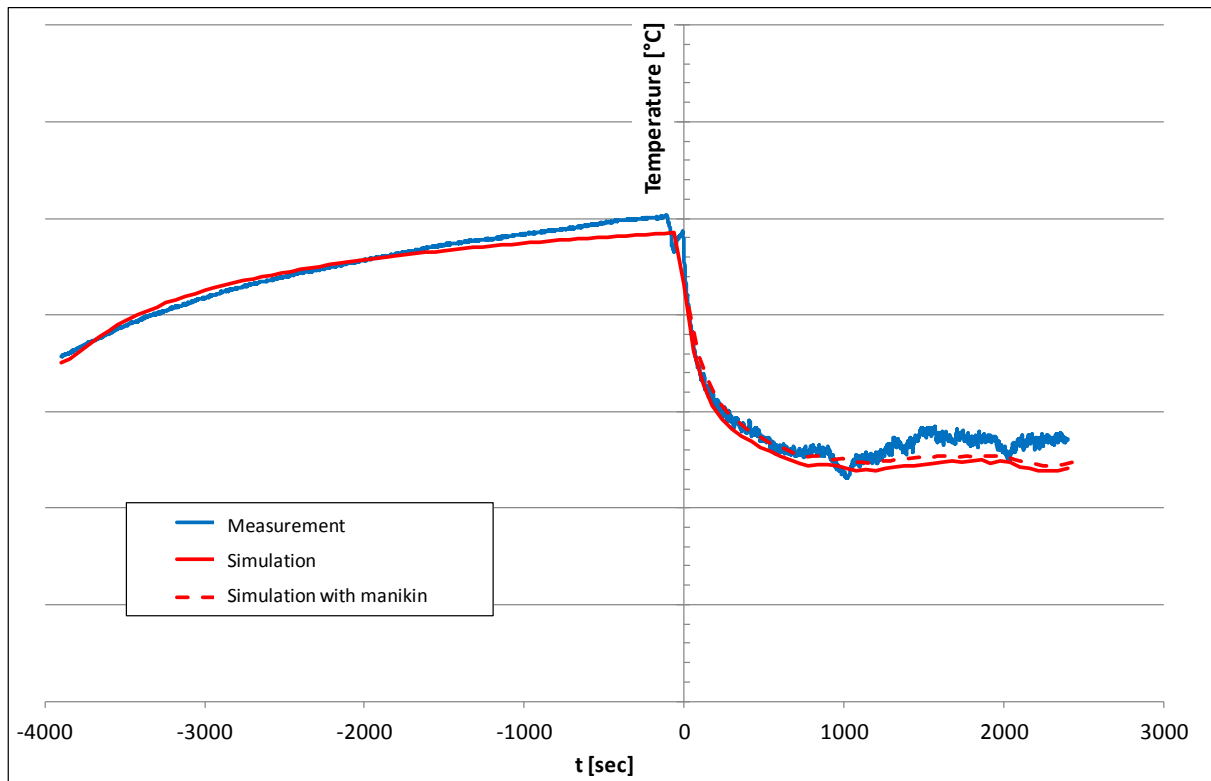


Figure 9: Temperature pull-down: comparison of average interior air temperatures (measured at the z-tube)

Measurements taken in environmental chamber tests included air temperatures taken at what is known as the “z-tube,” shown in figures 24 and 25. The tower accommodates a number of sensors that gauge the air temperature in the center of the vehicle cabin at regular intervals between the carpet and just below roof. The air temperature curves in figure 9 show the average z-tube temperatures, comparing actual measurements with simulation values. The two curves correspond extremely well. As illustrated in figure 5, the interior first heated up passively ( $t < 0$ ), i.e., the climate control system had not yet been switched on. Beginning at approximately  $t = 0$ , the blower fan is activated and cool air flows into the passenger compartment, quickly bringing the cabin air temperature to the target value. The volume flow was then reduced (see figure 5) to allow stationary, comfortable conditions to become established in the cabin, a set of conditions referred to as “pull-down.”

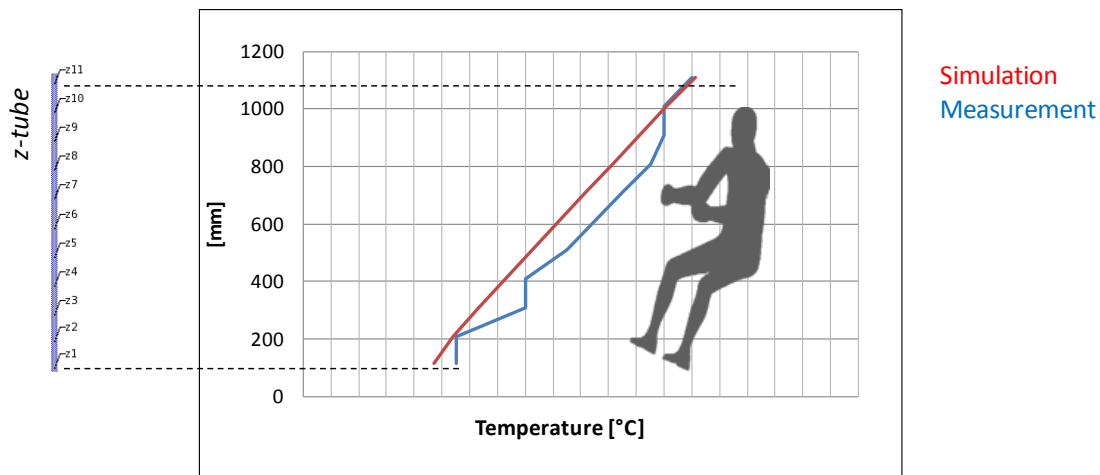


Figure 10: Temperature pull-down: comparison of interior air temperatures (measured at the z-tube) at  $t = 0$ .

The climate control system was not active during the passive heating phase ( $t < 0$ ), which results in what is known as temperature stratification, whereby the lower density of air heated by hot component surfaces causes it to rise up to just under the roof. As such, the air temperature in the footwell rises only slightly by comparison, and in our studies only increased by approximately  $5^{\circ}\text{C}$  after an hour of passive heating. Starting at the point when the air conditioner switched on ( $t = 0$ ), the air began to mix and stratification disappeared, i.e., the air temperature became homogeneous.

Quasi-stationary conditions were reached by the end of the pull-down phase, which means that the component temperatures (see figure 11) only underwent a slight change. As anticipated, the dashboard reached its highest temperature due to solar radiation through the windshield. The lowest temperatures in the cabin were measured at those surfaces that were not directly exposed to the light rays. The roof in particular was found to have very large temperature gradient: the temperature measured along the roof lining (interior) was on the order of the interior cabin air temperature. The temperature of the exterior metal sheeting, however, was high due to the absorbed solar radiation. On the whole, the large temperature gradient suggests that the thermal insulation in the roof is very good. Because no heat sources were defined within the overall e-Golf simulation model, the battery temperature, for instance, remained similar to that of the environmental air (see figure 11).

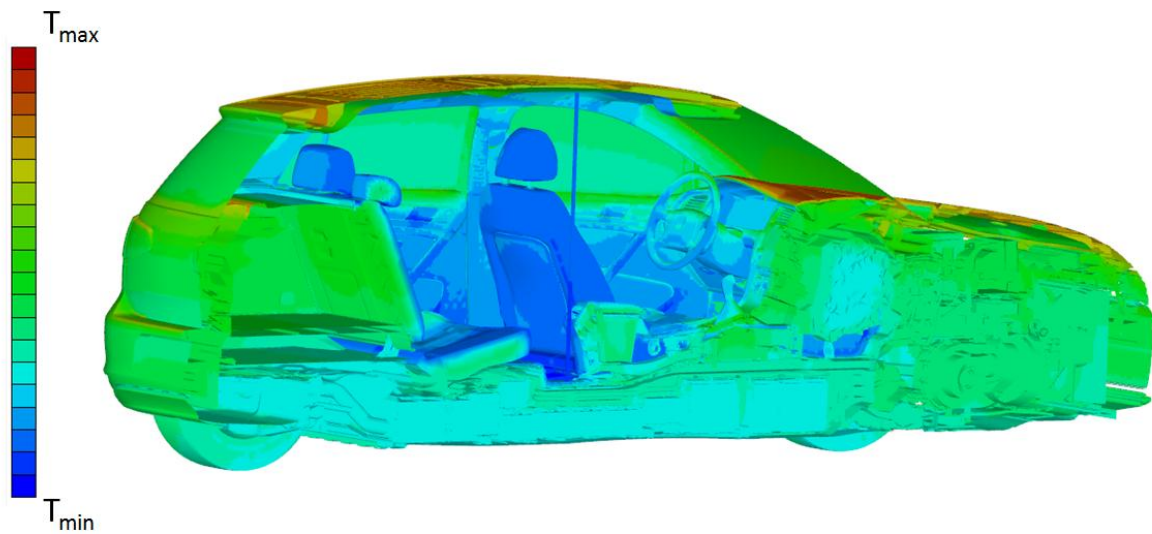


Figure 11: Temperature pull-down: temperatures of interior components at  $t_{\max}$

The validated basic model was then used to develop a series of variations for studying issues such as the degree to which perfect cavity insulation has an impact on the average calculated air temperature. This was done in the model by completely disregarding heat transfer within the small air cavities (see section 1): the simulated air temperature from figure 9 dropped off by no more than  $2^{\circ}\text{C}$  as a result. As indicated previously, heat is primarily exchanged with the environment via the windows. Future efforts to improve cabin insulation should not necessarily aim to continue enhancing insulation in cavities.

Another scenario that was simulated and tested was the use of uncooled external air to ventilate the passenger compartment during the passive heating phase (figure 9,  $t < 0$ ). Even though the external air was quite warm at  $35^{\circ}\text{C}$ , the  $50^{\circ}\text{C}+$  internal air produced a temperature delta that could be used for cooling of sorts. This was accomplished experimentally through the use of a solar-powered ventilation system. Upon comparison, the simulation and actual measurements were found to be in near perfect agreement, as shown in figure 12 (results are similar to those shown in figure 9). Passive ventilation reduced  $T_{\max}$  at  $t = 0$  by  $6 - 7^{\circ}\text{C}$ , which reduces the load on the climate control system for short trips. On longer trips, however, use of the air conditioning will reestablish stationary conditions essentially regardless of the starting conditions ( $t = 0$ ).

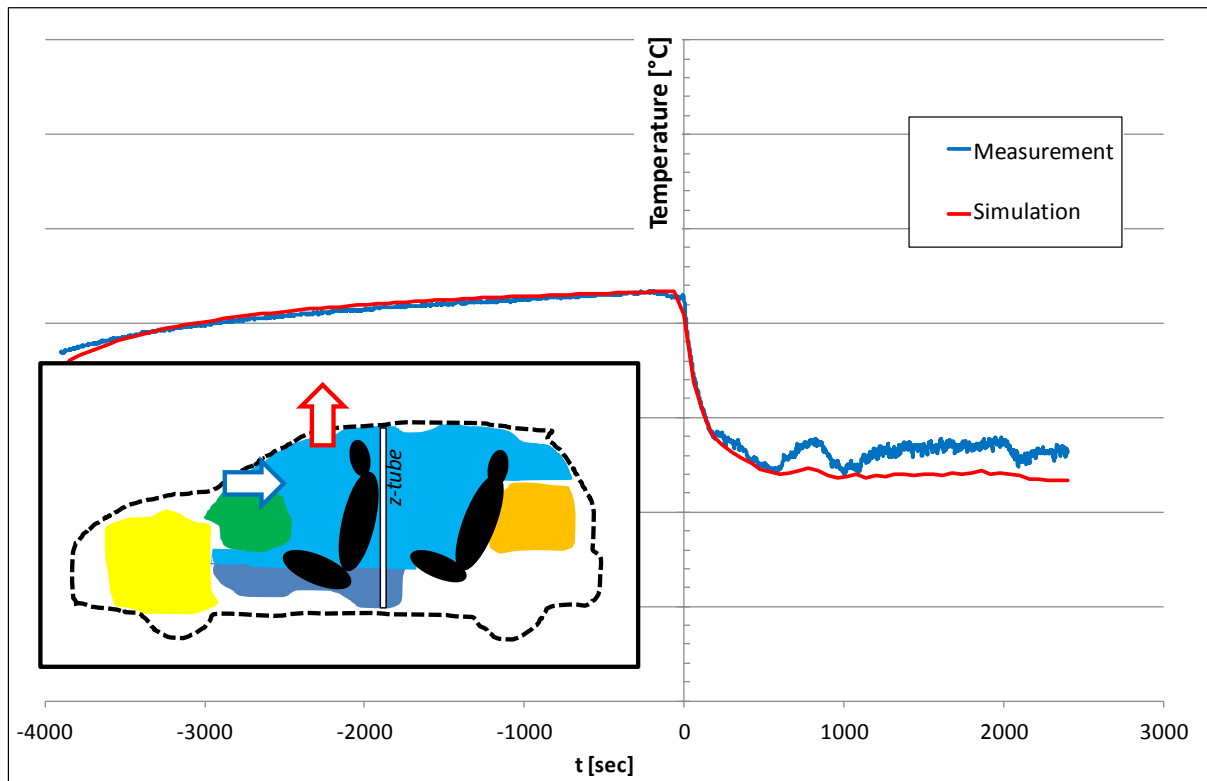


Figure 12: Temperature pull-down: comparison of average interior air temperatures (measured at the z-tube) with passive ventilation during the heating phase.

#### 4. Setup of a simplified thermal vehicle model for cabin simulation

Simplified cabin simulation models for designing climate control systems (such as INKA at BMW) have been known in the automotive industry since the 1990s and are now used in 1D thermo management tools (such as KULI, Flowmaster, etc.). In THESEUS-FE, the major difference from the detailed model lay in the significantly reduced geometry. Whereas the detailed model of the e-Golf (figure 11) contained a total of over 3 million surface elements, the generator model (figure 14) of the same vehicle consists of only 68 surface elements. The chassis/tires and engine compartment were not incorporated into this model, nor was the trunk. For the sake of simplicity, no thermal boundary conditions were defined at the interfaces with the omitted areas—these calculations were adiabatic, in other words. For the remaining contact surfaces within the cabin, however, the thermal boundary conditions applied were exactly the same as those used in the detailed model (figure 6). Solar and thermal radiation were taken into consideration both internally and externally<sup>8</sup>. For each FE, thermal conductivity was only calculated in the direction normal to the element. Unlike the

<sup>8</sup> In order to avoid energy conservation problems caused by the highly coarse mesh, the finite elements were further refined, i.e., divided into subelements, in THESEUS-FE Solver (internally).

detailed model, this model only mapped thermal conductivity in one dimension rather than in three; it did, however, apply a multilayer shell structure using the same material data used for the detailed model. An example is shown in figure 13.

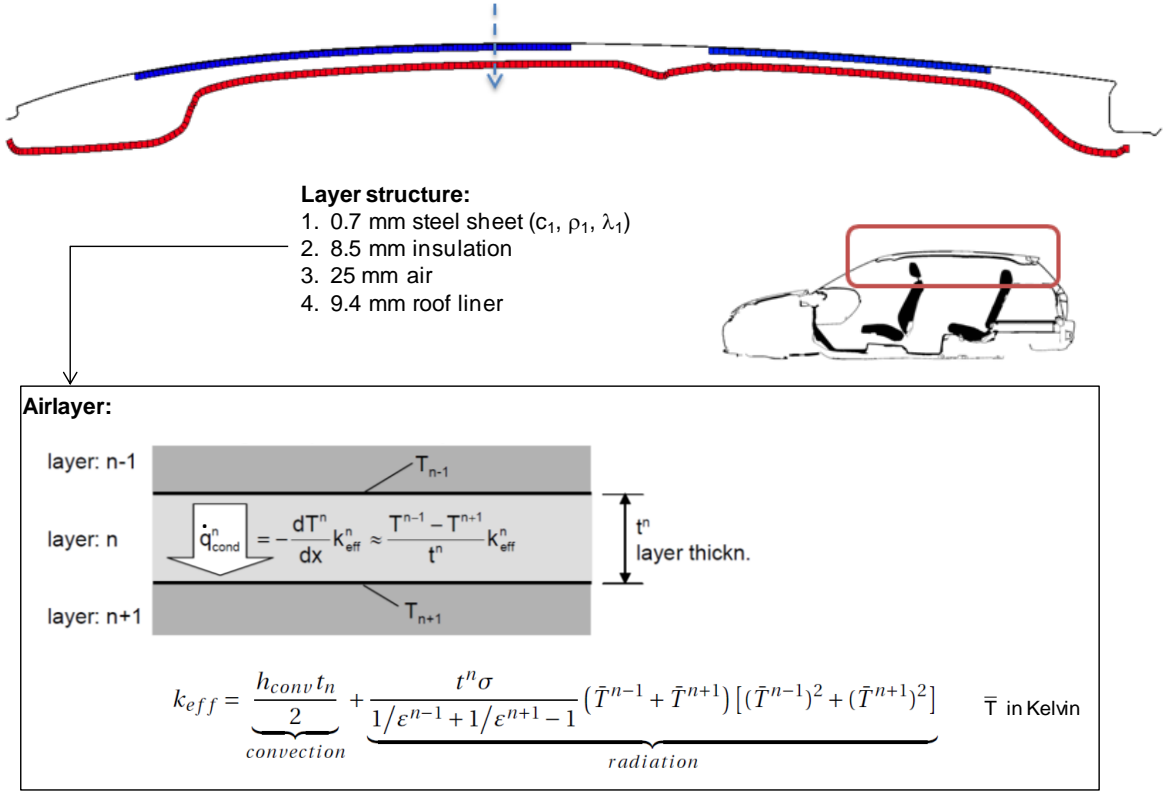


Figure 13: Shell structure for the roof in the 1D thermal conductivity generator model. Air layer definition [12].

In addition to the width of the vehicle, the finished generator model was created largely on the basis of the geometry points shown (in yellow) in figure 14, which could be defined as y-z coordinates.

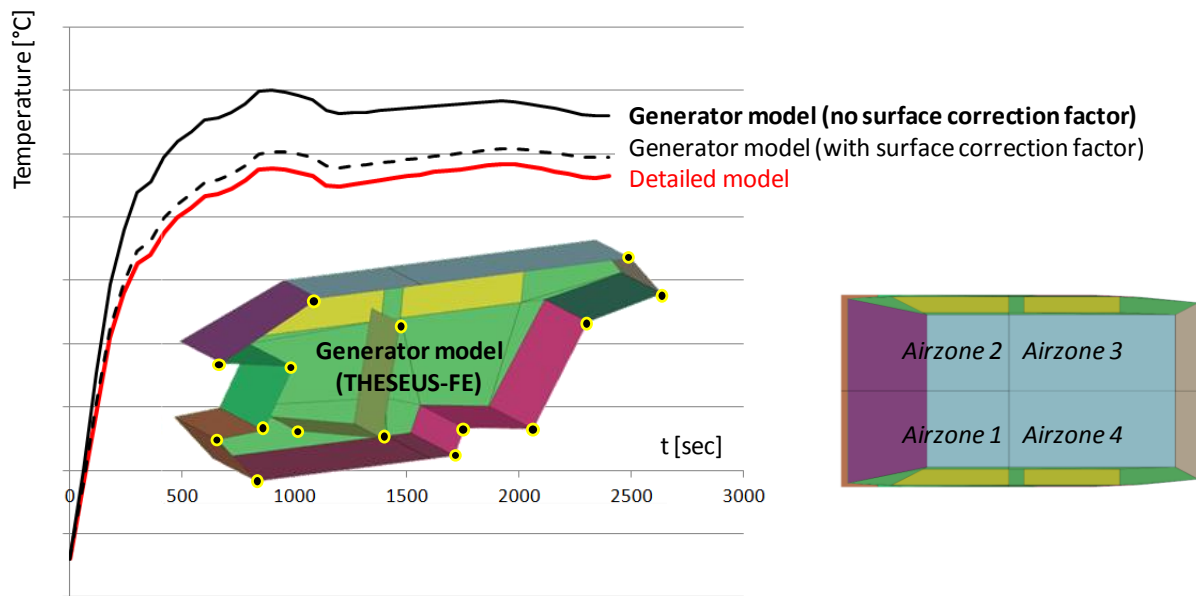


Figure 14: Generator model and simulation results (avg. air temp.) under winter load conditions

Because the project had a well-validated, detailed model at its disposal, we were able to improve the simplified generator model one step at a time. The quantities of heat introduced into the cabin were compared, for instance, as were the average component temperatures and, finally, the average cabin temperature in figure 14. Mapping the window surfaces and inclinations as precisely as possible was extremely important, especially with respect to the quantities of solar heat introduced into the cabin under summer load conditions.

Within the passenger compartment, properly modeling the convective heat transfer between components and the cabin air was one reason why we needed to introduce the following correction factor:

$$x = \text{real\_component\_surface} / \text{element\_surface}$$

Without this factor, the large, flat FEs in the generator model would frequently represent the surfaces in individual areas of the vehicle as being far too small. This was especially true for the seats, the floor and the door trim (interior), whereas the surfaces generally fit well for the roof and windows. In addition to affecting convection, the correction factor also had an impact on the mass and heat capacity of a given FE. As shown in figure 14, introducing an easily determined correction factor made it possible to significantly increase the quality of the simulation results from the generator model. As such, the painstaking, costly process of

setting up a detailed model can be eliminated going forward in cases where predicting the average interior air temperature under typical summer and winter load conditions is all that is needed. The reduction in computing time is especially worth noting, as the temperature pull-down requires

- 5 sec. of computing time for the generator model
- > 10 h of computing time for the detailed model.<sup>9</sup>

As shown in figure 14 (right), the edges of elements in a typical THESEUS-FE generator model are positioned in such a way that the cabin air temperature/humidity can be mapped from calculations involving no more than 4 air zones. Calculations involving more than one air zone require the user to define air exchange rates ( $dm/dt$  or  $dV/dt$ ) at zonal boundaries; the simulation also requires cabin airflow data to do this.

## 5. Simulating zonal climate control concepts under winter load conditions

The typical aim of cabin climate control is for the ambient temperature to become as homogeneous as possible in as short a time as possible. In typical automatic mode in the winter, for instance, warm air emanates from a variety of vents<sup>10</sup> simultaneously; this principle is illustrated in figure 15.

The basic idea underlying zonal climate control is to reduce energy consumption of the air-conditioning system simply by setting comfortable temperatures only in those zones that are actually occupied by passengers (figure 14, right). This concept is especially efficient for trips involving only one person (the driver) and for e-vehicles, which only have a limited energy reserve available to them.

An easy-to-remember parameter for describing this concept has been introduced in the literature [8]: *“...the zonal energy efficiency ratio, or ZEER, is defined as that portion of the total interior load required for keeping the environment static relative to the target value in the occupied zones of the vehicle interior. The ZEER value lies between 0 and 1, and provides information on the amount of energy that the OZ system<sup>11</sup> saves compared to a traditional HVAC system.”* If an interior climate control system variation has a ZEER of 0.5, for example,

---

<sup>9</sup> Computing time corresponds to a traditional Linux or Windows machine on a single CPU.

<sup>10</sup> For the sake of simplicity, the defrost vent along the windshield (below) was not considered here.

<sup>11</sup> The OZ (occupied zones) system only heats and/or cools those cabin zones where passengers are seated.

this means that the system requires half the energy of classic vehicle heating and cooling systems.<sup>12</sup>

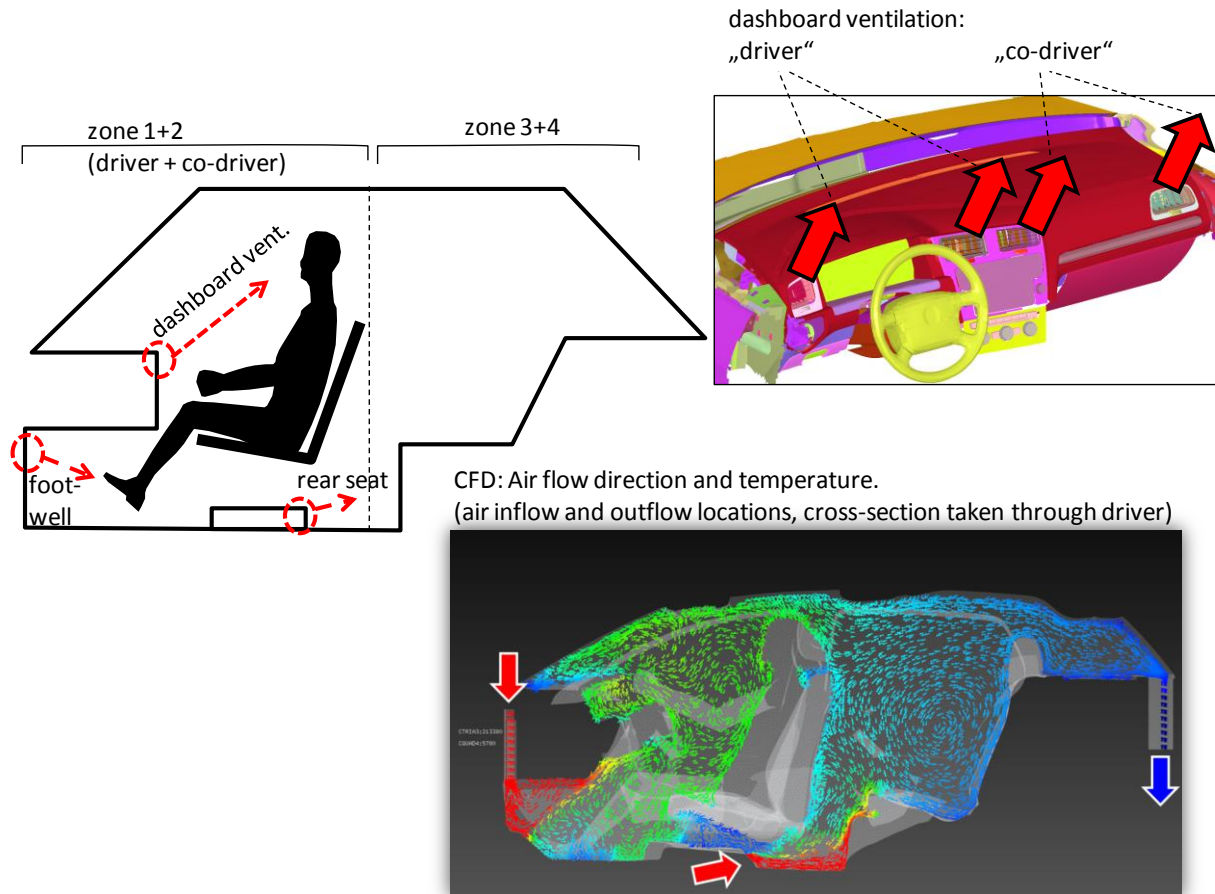


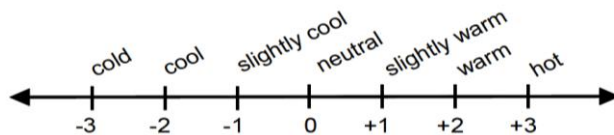
Figure 15: Cabin climate control under winter load conditions (below: CFD results)

The generator model can be operated in the simulation with up to 4 air zones, and was used in the E-Komfort project to estimate the potential energy savings generated by zonal climate control concepts. This involved the following simplifications and conventions:

- It is assumed that the cabin airflow is stationary. For this reason, the volume flow at zonal boundaries was calculated in advance using stationary CFD analyses in OpenFOAM. As a result, the temperature ( $T_{in}$ ) and the total volume flow ( $dV/dt$ ) of the warm air entering the cabin is taken to be approximately constant over time.
- A total of 3 zones were used. Air zones 3 and 4 (in figure 14) were combined into a single zone (see figure 17).

<sup>12</sup> The classic vehicle interior climate control system will be referred to as the “base model” in the following.

- The goal of each variation was to bring the average air temperature in the driver's zone up to a comfortable<sup>13</sup> 24.7°C after 10 minutes.
- The PMV index was used for assessing global thermal comfort in the driver's zone for the base model and for all variations. Across the board, PMV values fell in the  $-1 < \text{PMV} < 0$  range for the base model and for all variations after 10 minutes. Because this is close to what is considered neutral, it was rated "comfortable."



- The unknown variable in every simulation was the temperature of the warm air entering the cabin ( $T_{in}$ ) needed to reach this goal within 10 minutes. The net performance for operating with outside air was then calculated as proportional to the temperature difference ( $T_{in} - T_0$ ).
- The ambient air temperature under winter load conditions remained constant at  $T_0 = -7^\circ\text{C}$ .
- In addition to the constant volume flows at zonal boundaries, the average air speeds per zone were also taken from the (stationary) CFD simulation. These values were used in the generator models to simulate heat transfer between zones and the wall. Volume conservation was tested for each zone, i.e., all volume flows into and out of the cabin had to add up to 0. Given the small temperature differential, this meant that mass was (approximately) conserved.

Overall, variations 1 – 3 were simulated with generator models (see section 4) along with the base model. Figures 16 and 17 show the general boundary conditions for the climate control system and the results.

---

<sup>13</sup>An average air temperature of 24.7°C may seem somewhat high. It is important to keep in mind, however, that components/windows were still cool after 10 minutes, resulting in a significant loss of heat through radiation, which had to be offset with a higher ambient temperature. A radiation background temperature of 19.3°C and an ambient temperature of 24.7°C produced what is referred to as an operative temperature of 22°C (on average).

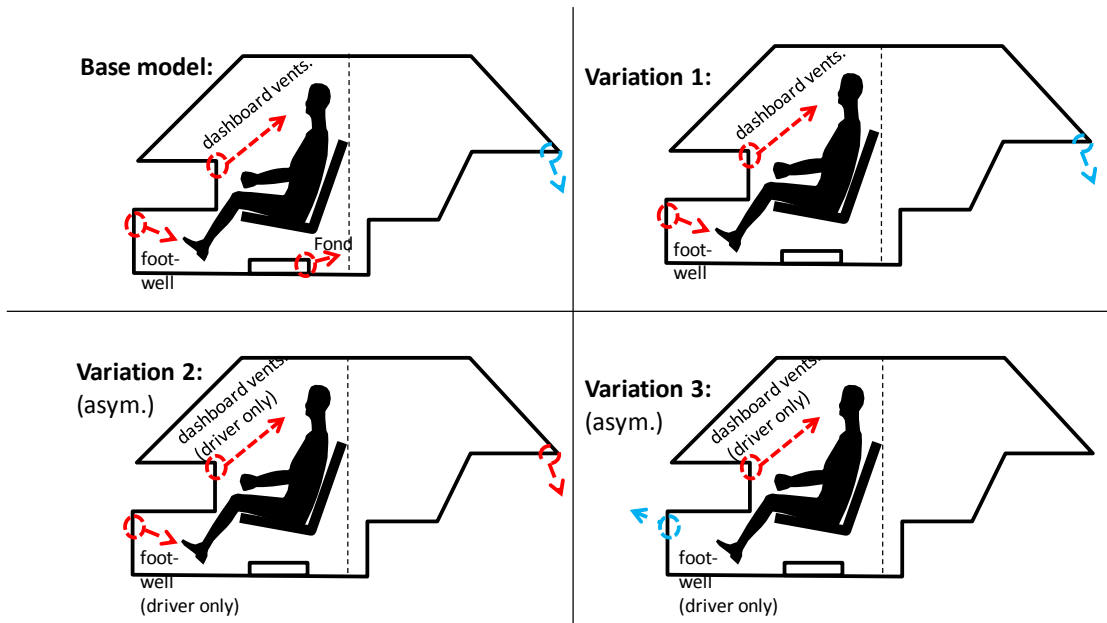


Figure 16: Zonal climate control variations: inflow and outflow locations (winter load)

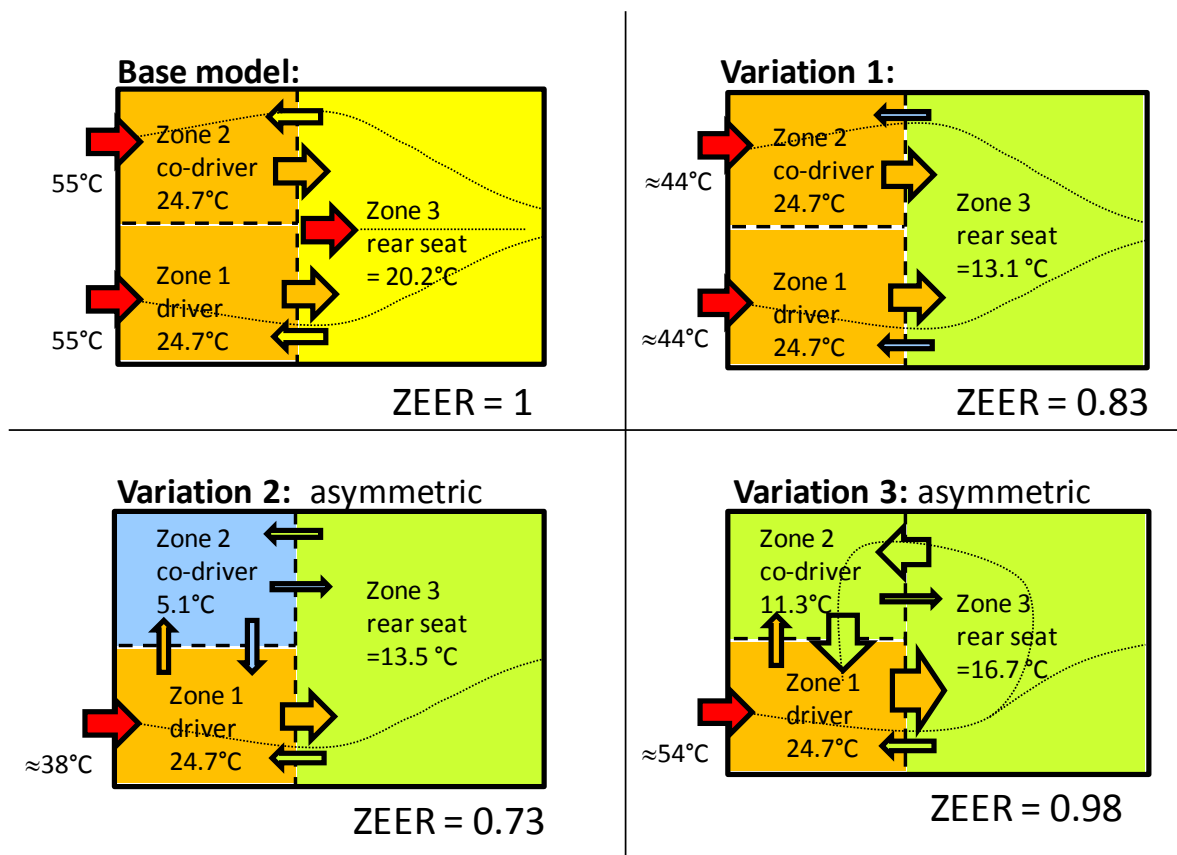


Figure 17: Zonal climate control variations: results after t = 10 min. (winter load)

The total volume flow (in  $\text{m}^3/\text{s}$ ) for all inflow vents was identical to that of the base model for all variations. This made it possible to extrapolate the energy efficiency of each scenario on the basis of the temperature of the air entering the cabin. The temperatures for the base model and for variation 3 were nearly identical, resulting in a ZEER value of  $\approx 1$ . The difference between variations 2 and 3 can be seen in figure 16: in one scenario, air flowed into the cabin in the footwell, and in the other scenario air flowed out through the footwell. As figure 17 shows, warm air in variation 3 was blown into the cabin through the dashboard air vents, transported through the cabin counterclockwise and then drawn off through the driver's side footwell. This method was found to be ineffective, however, yielding a ZEER of  $\approx 1$ . Introducing air through the dashboard and front floor vents and drawing it off through the rear of the vehicle proved to be much more effective.

Finally, all of the variations mentioned here were assessed in coupled simulations as well. The primary features of this kind of fully coupled simulation will be discussed in subsequent sections.

## **6. Comfort simulation with infrared emitter models**

The E-Komfort project involved conducting what are known as coupled simulations, in which comfort is assessed by applying local thermal comfort indices to human models in the THESEUS-FE software on the one hand, and by performing special cabin air flow simulations on human occupants. These methods were used as a way of monitoring whether local thermal conditions were comfortable when applying zonal climate control concepts (section 5). Infrared emitters<sup>14</sup> were also used for cabin simulations of winter load conditions in order to reduce the temperature of air entering the cabin and increasing energy efficiency still further.

Because evaluating local comfort involved taking a detailed look at the effect of air flow and temperatures on occupants, the CFD analyses were carried out in OpenFOAM and coupled with THESEUS-FE. A more in-depth discussion of coupling will be provided beginning in section 7, at which point the results of coupled simulations will be validated.

Discussion in the current section will center on the physical phenomena that were taken into account in the coupled simulation:

- Forced and free cabin airflow with OpenFOAM

---

<sup>14</sup> Infrared emitters emit wavelengths  $> 750 \text{ nm}$ , which is just beyond the visible spectrum (380 – 750 nm).

- Convective heat flow data from OpenFOAM were applied in THESEUS-FE as boundary conditions for each FE.
- Wall temperatures from THESEUS-FE were defined as boundary conditions in OpenFOAM
- FIALA-FE<sup>15</sup> is a thermo-physiological model that takes thermal conductivity in humans into consideration, as well as blood flow, metabolism, shivering, contact heat, clothing, breathing, evaporation and perspiration (and moisture exchange in OpenFOAM). The flow of heat caused by radiation and convection was applied to sector surfaces in W/m<sup>2</sup>.
- Thermal comfort assessment<sup>16</sup> for the FIALA-FE human model: PMV, DTS, equivalent temperature, ISO-14505-2, Zhang
- Using THESEUS-FE for 3D thermal conductivity in components
- 3D radiation, long- and shortwave, in THESEUS-FE

One challenge faced in the project was mapping infrared emitters in the simulation. This meant having to revise ray tracing in THESEUS-FE in a way that would also allow us to model reflection from reflective surfaces (see figure 18).

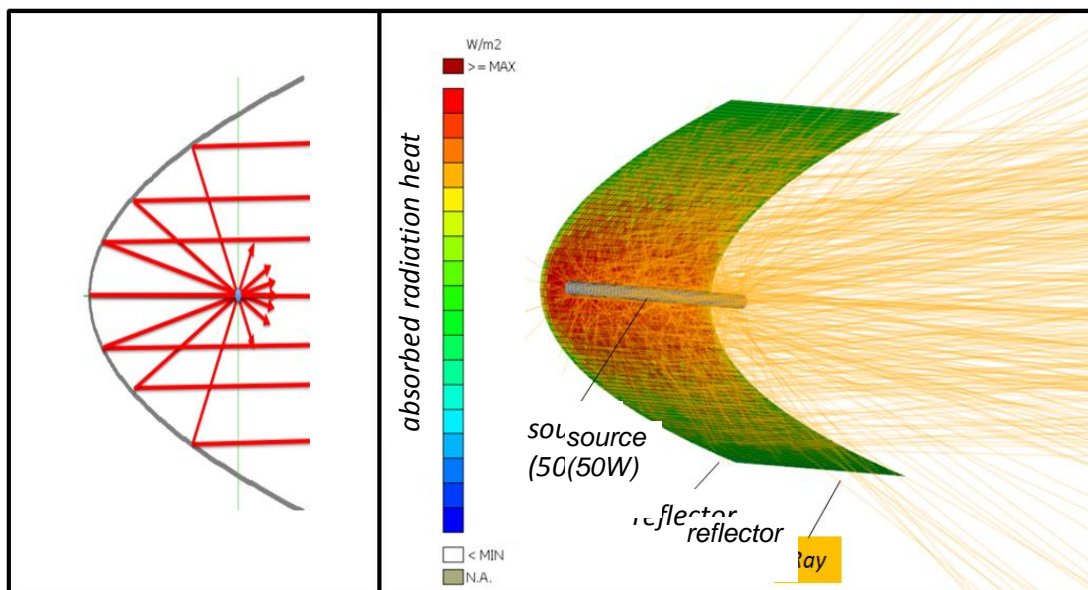


Figure 18: Infrared emitter with reflector in THESEUS-FE

If the user defines the source as 50 W, for instance, this radiation is distributed evenly over all surface elements of the source. Each surface element reflects the energy in the form of

<sup>15</sup> FIALA-FE is a thermal human model fully integrated into THESEUS-FE, based on [2].

<sup>16</sup> See [1], [2], [4], [5], [11] and [12]

photons, which are then carried into the room in large numbers. The points where the photons ultimately make contact can be seen in figure 19.

*Winter load conditions:*

*Heating, inflow temperature reduced:*

• Base model with no IR emitter

• Version with 2 IR emitters

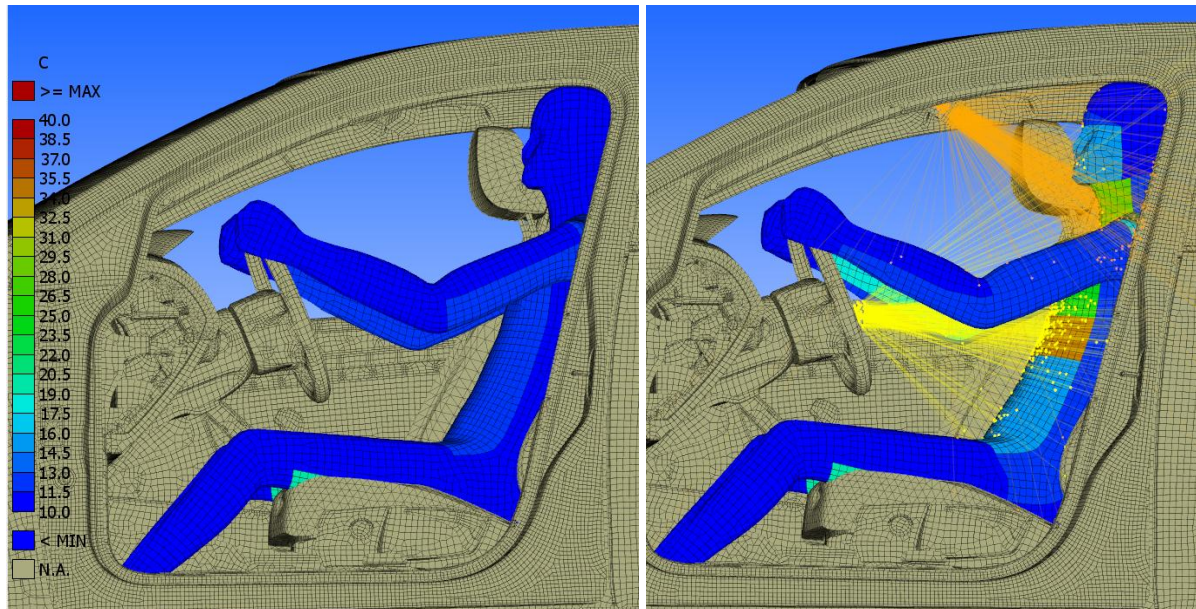


Figure 19: Equivalent temperatures after  $t = 10$  min.

The simulation had to be carried out with a large number of photons in order to make as accurate a prediction as possible of the radiant heat coming into contact with each manikin FE and to avoid gaps in results between elements. Note that the photon beams shown in figure 19 are only a fraction (1 in 1000) of the actual number of photons simulated.

In some variations (such as shown on the right in figure 19), the aim of simulations was to determine how much additional heat IR emitters could transfer to the human model under winter load conditions when the inlet air temperature has been reduced. The goal was for the radiation to affect as large a surface area as possible, which could be effected by optimizing the positioning, power and reflector geometry of the IR emitters in the simulation. At the same time, the equivalent temperature and/or thermal comfort were monitored so that the heat introduced would not be assessed as uncomfortable. The background for equivalent temperature is comparable to that of the wind chill factor used when forecasting cold weather conditions, whereby the actual heat flow (in  $W/m^2$ ) at a surface is transferred to an ideal space tempered to a uniform temperature  $T_{eq}$ . The physical conditions within the ideal space are homogeneous:

- No forced movement of air ( $v_0 = 0$  m/s)

- Air temperature  $T_0 = T_{eq}$
- Background radiation/ wall temperature: uniform at  $T_w = T_{eq}$

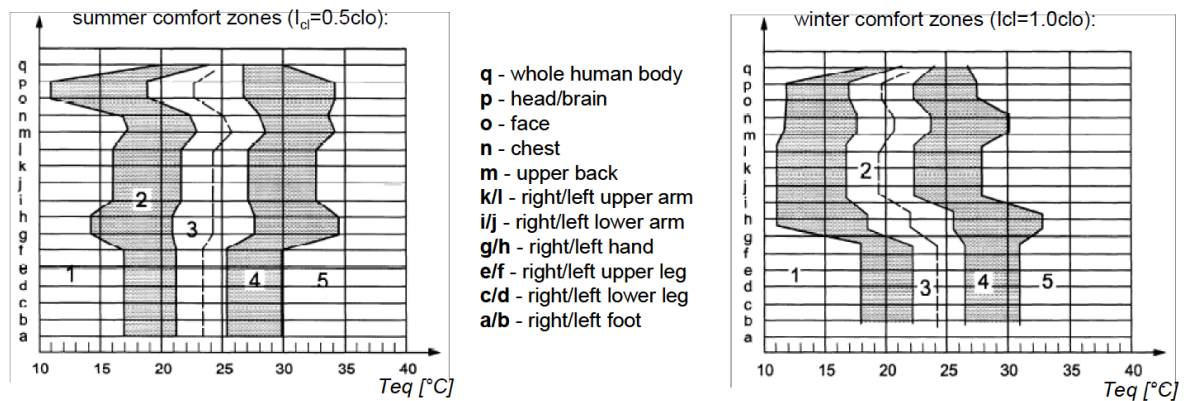
Setting the actual heat flow<sup>17</sup> equal to that in the ideal space allows us to solve for  $T_{eq}$ :

$$\dot{Q}_{real} = \dot{Q}_{eq}(T_{eq}) \rightarrow T_{eq}$$

The sectors of the human surface/skin shown in figure 19 exhibiting the highest equivalent temperatures are those in contact with the most photons per unit area and/or the highest infrared heat flow. Achieving the same heat flow along these surfaces in the ideal space requires heating the space to a relatively high equivalent temperature.

The concept of equivalent temperatures, in other words, allows us to convert complex heat flow data in  $W/m^2$  (which may have a variety of components, such as thermal radiation and convection) to temperatures that are easy to work with and intuitively meaningful.

In the subsequent step, we were able to use the local equivalent temperatures as a basis for deriving local comfort indices for each area of the body (as described in ISO-14505-2).



1 - to cold (uncomfortable), 2 - cold, but comfortable, 3 - neutral, 4 - warm, but comfortable, 5 - to warm (uncomfortable)

Figure 21: Defining the comfort zones described in ISO-14505-2 for summer and winter load conditions

This, in turn, allowed us to evaluate the energetic impact of various simulated scenarios having a local effect. The aim of these simulations was always to avoid heating or cooling the entire cabin, as is conventionally done.

The following sections will take a more in-depth look at coupling between THESEUS-FE and OpenFOAM.

<sup>17</sup> The actual heat flow is taken from the simulation.

## 7. Motivation for using coupled simulations

A number of coupled heat exchange processes take place in the passenger compartment's thermal system.<sup>18</sup> Predicting the local perception of comfort depends on the temperature of the adjacent air, the movement of air and the net thermal radiation at individual areas of the body. Obtaining these data means having to predict the local air-flow conditions with precision.

This is done using a co-simulation; the physical problem, in other words, is divided into multiple constituents, each of which is modeled separately using specialized simulation programs. To guarantee coupling between these constituent areas, data - typically boundary condition parameters - were exchanged continuously after each time interval or iteration.

The following are some disadvantages to this approach:

- Potential numerical convergence problems if coupling is too loose - direct heat flow transfer, for instance, can destabilize the co-simulation.
- Data transfer and the need for an external mechanism for synchronizing multiple programs make co-simulation more time-consuming.
- Interpolation errors arise if fields such as local surface temperature need to be transferred between different computer networks.

The approach also offers the following advantages, however:

- Each simulation tool can be assigned to a matching and/or natural subprocess; modeling an air conditioner is a common example of this. Local details, such as flow in channels or heat exchangers, are not of interest for simulating the passenger compartment. Using a CFD tool for 3D modeling is also impractical; a simplified, 1D network can be used for modeling an air conditioner instead, exchanging data with the 3D cabin flow model via a suitable interface. Modeling human physiology and comfort information is another example of this advantage: very few tools (THESEUS-FE is one) are capable of delivering the kind of detailed, well-validated information on the impact of human occupants on the thermal system. Our practical experience has also shown that no single CAE tool is capable of generating a comprehensive model of all important thermal effects. Sophisticated simulations (of the passenger compartment, in this case) often require falling back on coupled computing.
- This approach gives users considerably more modeling flexibility. Decoupling a submodel from the overall system is quite simple, for instance - in other words, users can freeze the boundary conditions in the as-delivered state. In the example of an air

---

<sup>18</sup> See figure 6.

conditioner, this means that users could dispense with performing additional network simulations once the air temperature has leveled off to a constant value at vents directing air out of the cabin - doing so can cut computing time. Another option that we have already taken advantage of in our practical work is to generate separate simulations of air circulation outside the vehicle. The results of these simulations can be applied as frozen parameters describing convection boundary conditions for a thermal simulation of the passenger compartment.

### 8. Coupling strategy for the passenger compartment

The coupling plan shown in figure 22 was used for creating a thermal simulation of the cabin. The basic premise was to divide the system into cabin air (OpenFOAM) and solid components (THESEUS-FE), with THESEUS-FE also modeling the radiant heat transfer between surfaces. Optional simulation components include integration of human thermal models for passengers, consideration of local water vapor transport in the cabin air, and possible network models for air-conditioner performance.

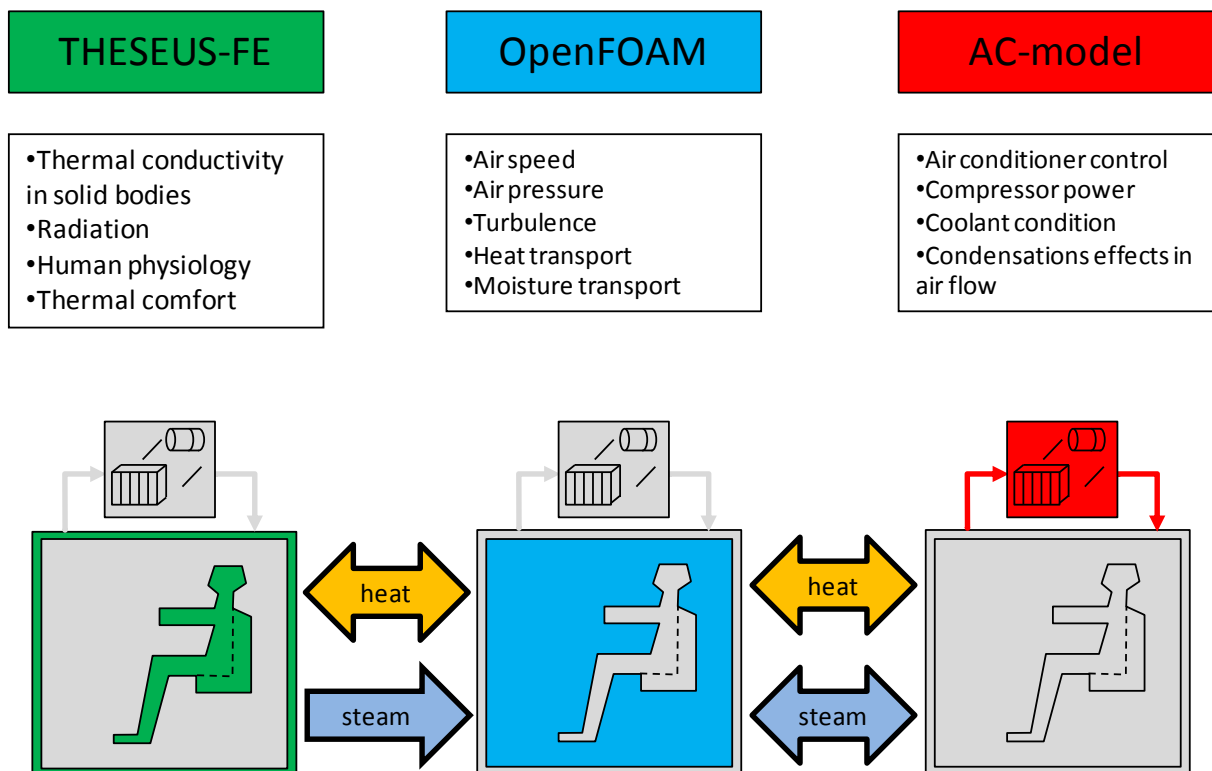


Figure 22: Coupling plan for cabin simulation

Coupling between the THESEUS-FE and OpenFOAM models (indicated in figure 22 by the arrows between the left and center system) consists of convective heat exchange between

solid bodies and adjacent air masses. Heat at these couplings can flow in both directions depending on whether the climate control system is being used for heating or cooling. The role that seats and other add-ons play as thermal reservoirs in the cabin must always be taken into consideration; subsequent heating or cooling of solid components often has a considerable impact on the temperature of the cabin air. Using passenger models in THESEUS-FE (figure 23) allows users to account for water vapor produced by breathing and evaporation from the skin. This effect is unidirectional (bottom blue arrow to the right), as occupants act only as a source of water vapor, and the model does not currently take local absorption or condensation of water vapor into account.

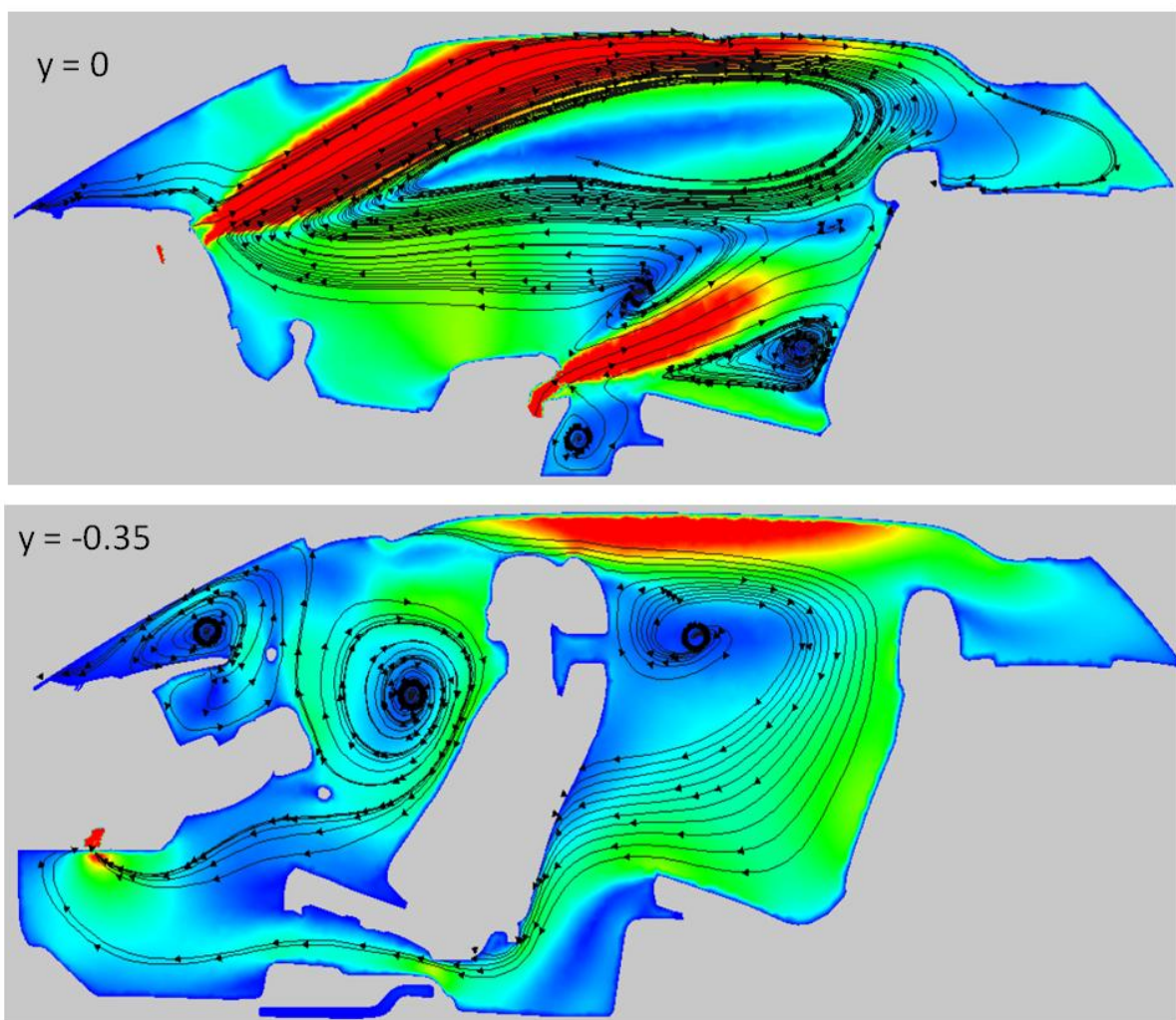


Figure 23: Cross-sectional model showing the effects of an occupant on air speeds ( $y=0/-0.35$ )

In the OpenFOAM model, inflow and/or outflow boundary conditions can be used for directly modeling air conditioner performance in simple scenarios. This typically requires knowing the

inflow temperature, mass or volume flow data, and the moisture level of the air entering the cabin. Integrating an additional air conditioner model lends itself well here, as these parameters often vary over time and are not known advance. In this scenario, models of this kind yield inflow parameters in OpenFOAM; when operating with recirculated air, by contrast, they can incorporate the temperature and humidity level of the cabin air at exhaust points. Of particular interest here is the treatment of convective heat exchange between solid bodies (in THESEUS-FE) and cabin air (in OpenFOAM). THESEUS-FE typically uses convection boundary conditions at all component boundary points in keeping Newton's Law of Cooling,

$$\dot{q}_{TFE,conv} = h_{TFE}(T_{TFE,fluid} - T_{TFE,wall})$$

whereby

- $\dot{q}_{TFE,conv}$  = convective heat flow into the component, measured in W/m<sup>2</sup>
- $h_{TFE}$  = local heat transfer coefficient, measured in W/(m<sup>2</sup>K)
- $T_{TFE,fluid}$  = adjacent temperature in °C
- $T_{TFE,wall}$  = local component temperature in °C

Parameters  $h_{TFE}$  and  $T_{TFE,fluid}$  are entered by the user, while component temperature  $T_{TFE,wall}$  is calculated as part of the THESEUS-FE solution. This means that the convective heat flow is always implicitly dependent on the current temperature of the component. Linearizing the convective heat flow in this way is ultimately a model assumption and only makes sense if the heat transfer coefficient and fluid temperature are defined consistently.

The  $h_{TFE}$  and  $T_{TFE,fluid}$  field variables vary over space and time in the context of transient coupled simulations. THESEUS-FE delivers wall temperature  $T_{TFE,wall}(t_n)$  at time interval  $t_n$ , which our mapping method interpolates into the OpenFOAM network. For the subsequent time interval in OpenFOAM, the resulting field  $T_{OF,wall}(t_{n+1})$  then serves as a new Dirichlet boundary condition for the temperature transport equation. When combined with the wall treatment in the selected turbulence model, the finite volume method underlying OpenFOAM calculates heat flow  $q_{OF,conv}(t_n)$  along the wall from  $T_{OF,wall}(t_n)$  and the current temperature solution  $T_{OF,fluid}(t_n)$  in cells near the wall. This is then used in

$$h_{OF}(t_n) := \dot{q}_{OF,conv}(t_n) / [T_{OF,fluid}(t_n) - T_{OF,wall}(t_n)]$$

to determine a local heat transfer coefficient on the OpenFOAM side. The OpenFOAM network maps variables  $T_{OF,fluid}(t_n)$  and  $h_{OF}(t_n)$  onto the THESEUS-FE network, where they become  $T_{TFE,fluid}(t_{n+1})$  and  $h_{OF}(t_{n+1})$ , acting as parameters for convection boundary conditions in the subsequent step. While a conceivable alternative would be to directly stipulate an interpolated convective heat flow  $q_{TFE,conv}$  as a boundary condition in THESEUS-FE, this method was found to readily lead to numerical instability.

Parameter	Units	Source	Target	
Wall temperature $T_{wall}$	°C	THESEUS-FE	OpenFOAM	field
Local convective coefficient of heat transfer $h$	W/(m <sup>2</sup> K)	OpenFOAM	THESEUS-FE	field
Adjacent fluid temperature $T_{fluid}$	°C	OpenFOAM	THESEUS-FE	field
Current time increment $\Delta t$	S	THESEUS-FE	OpenFOAM	scalar
Rate of water vapor generation $J$	kg/(m <sup>2</sup> s)	THESEUS-FE	OpenFOAM	field
Mass fraction of water vapor $Y_{H_2O}$	-	OpenFOAM	THESEUS-FE	field
Air pressure $p$	Pa	OpenFOAM	THESEUS-FE	field
Avg. inlet temperature $T_{in}$	°C	AC model	OpenFOAM	scalar
Avg. water vapor fraction $X_{H_2O,in}$	-	AC model	OpenFOAM	scalar
Avg. outlet temperature $T_{out}$	°C	OpenFOAM	AC model	scalar
Avg. water vapor fraction $X_{H_2O,out}$	-	OpenFOAM	AC model	scalar
PMV (=global comfort index)	-	THESEUS-FE	AC model	scalar

Table 1: List of variables exchanged by the THESEUS-FE coupler

The transfer of a PMV value (Predicted Mean Vote, a comfort index defined in DIN EN ISO 7730) in the last line of table 1 refers to potential new concepts for regulating climate control systems. The traditional goal when regulating a climate control unit is to achieve and maintain a desired average cabin temperature, i.e. one that acts as a rough measure of passengers' thermal comfort. An alternative here would be to define the goal as quickly achieving a neutral level of passenger comfort.

One concrete option would be to take a PMV value that THESEUS-FE determines for the driver and send this information directly to the climate control model. A simulated PMV controller in the climate control system would then adjust the current temperature of air blown into the cabin in order to maintain a neutral PMV.

The mathematical model underlying this alternative assumes a current error  $e$  between the target and actual value:

$$e(t) = 0 - PMV(t).$$

In this scenario, the target value,  $PMV = 0$ , corresponds to optimum comfort. The control unit then generates an output signal

$$u(t) = R[e(t)].$$

This signal is used for adjusting the outflow temperature of the climate control system:

$$\frac{d}{dt}T_{out}(t) = u(t).$$

There are three different components of a PID controller:

$$R[e(t)] = K_p e(t) + K_i \int_0^t e(\tau) d\tau + K_d \frac{de}{dt}(t)$$

These are known as the proportional, integral and/or differential terms. Careful selection of these three coefficients allows users to optimize the response without overshooting the target.

## **9. Validating the coupled cabin simulation**

The aim of environmental chamber measurements was to validate the coupled simulation methods described above for calculating temperatures in the vehicle cabin.

The load case studied was a simplified pull-down scenario. Temperature sensors were installed at a series of air test points within the cabin, and a vertical tube was installed in the backseat area to create a number of additional test points spanning the height of the vehicle. We overrode the control unit, forcing the system to run constantly at the highest fan speed after it was turned on. This was followed by conditioning the vehicle in the environmental chamber at a temperature of 35°C. We then activated the air conditioner at  $t = 0$  s and observed temperature measurements over the course of an hour. In studies leading up to this, the resulting volume flow was measured separately at all inlet vents. A 10 km/h flow of 35°C air was maintained outside the vehicle. Solar loads and passengers were neglected in this study in order to keep the experimental conditions as clear and simple as possible. The air conditioner was only run in recirculation mode for the cooling phase.

The simulation was conducted as a two-stage process:

- The first step was to calculate the stationary flow field, using the volume flow rates at the inlet vents as boundary conditions. The flow is “cold,” which is to say that energy transport was not taken into consideration.
- The speed and pressure fields calculated in step 1 were frozen along with the state of turbulence and used as fixed values from that point onward. We then used a coupled THESEUS-FE/OpenFOAM simulation as described above to calculate the transient development of the temperature field for the cabin air and for components over the course of an hour.

This method is suitable for flows comprised primarily of forced convection, in which the forces of buoyancy and the effect that temperature fluctuations have on the flow rate are negligible. Finding an exclusive solution on the CFD side of the (linear) energy transport equation allows for relatively large time intervals and fast computing times. Users could typically generate this kind of coupled simulation on a simple workstation without parallelization, completing the task over the course of a day.

Figures 24 – 29 show examples of transient temperature curves at the test points at which measurements were taken. The curves for the simulated temperatures were found to agree quite well with those of measured temperatures, demonstrating that the use of coupled models is a relatively precise method for determining local air temperatures in the vehicle cabin.

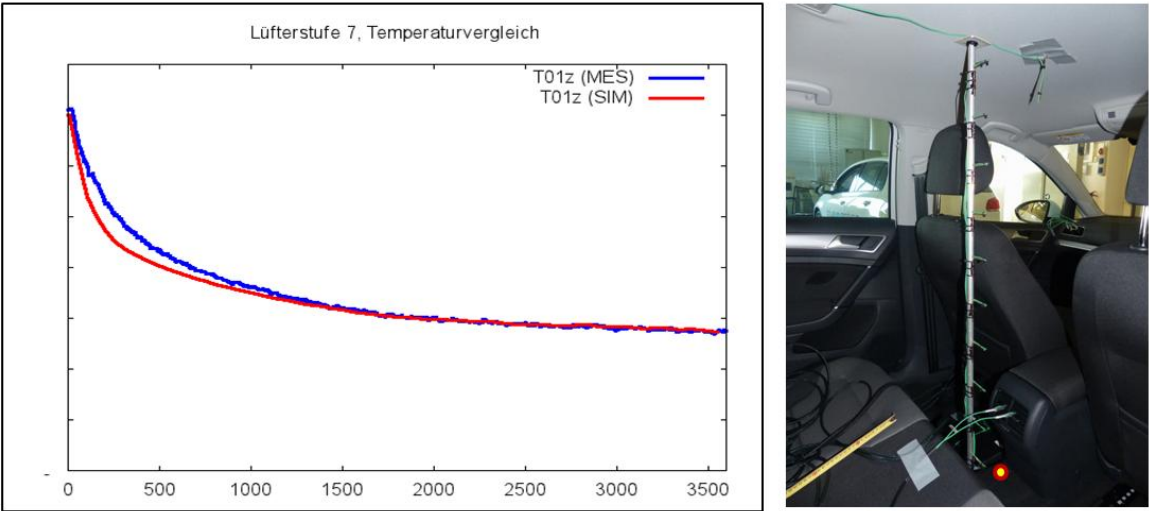


Figure 24: z-tube test point (T01z)

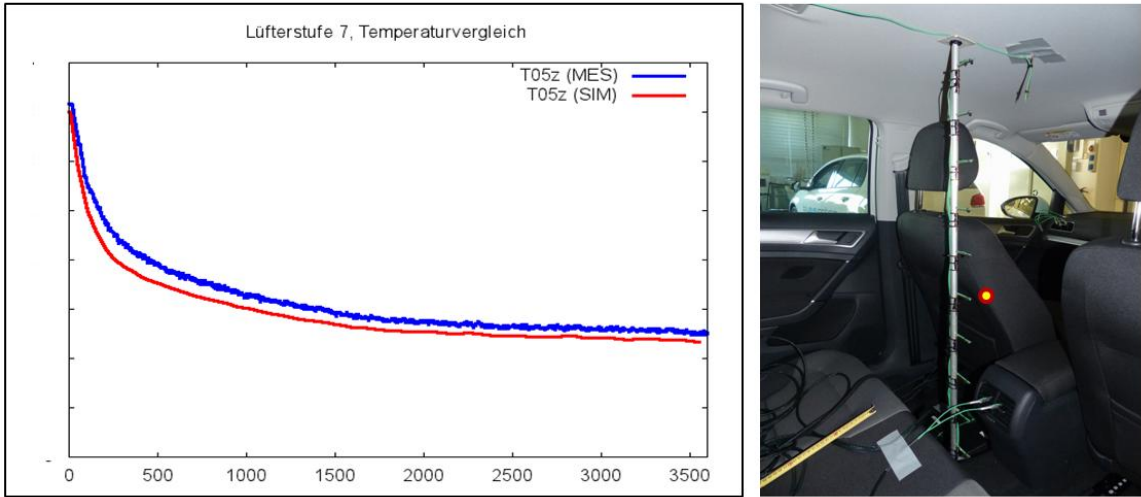


Figure 25: z-tube test point (T05z)

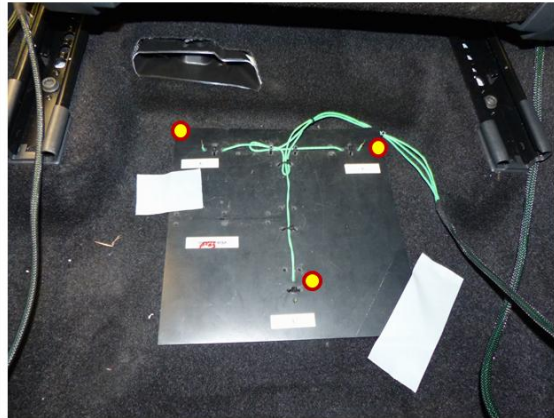
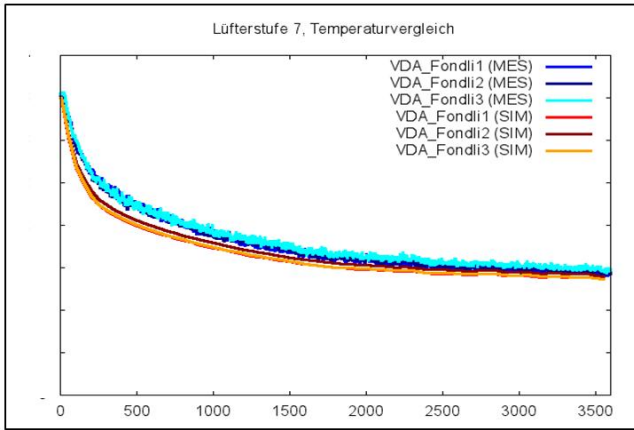


Figure 26: Test points in the rear footwell (left)

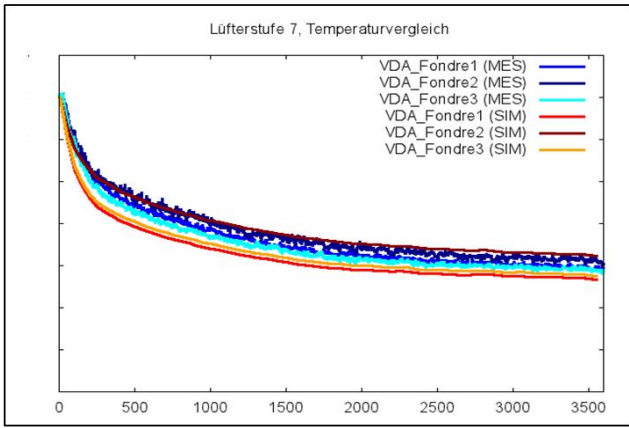


Figure 27: Test points in the rear footwell (right)

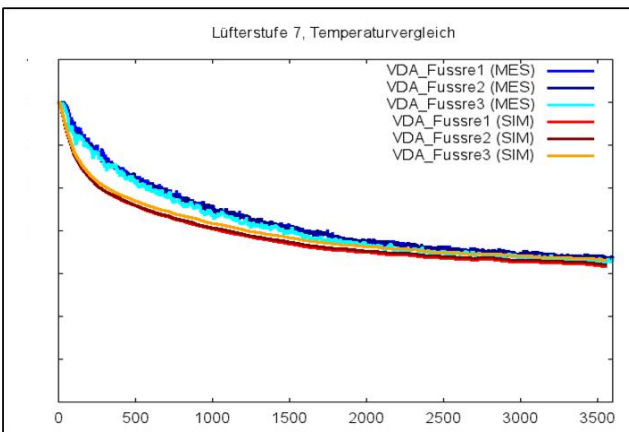


Figure 28: Test points in the front footwell (left)

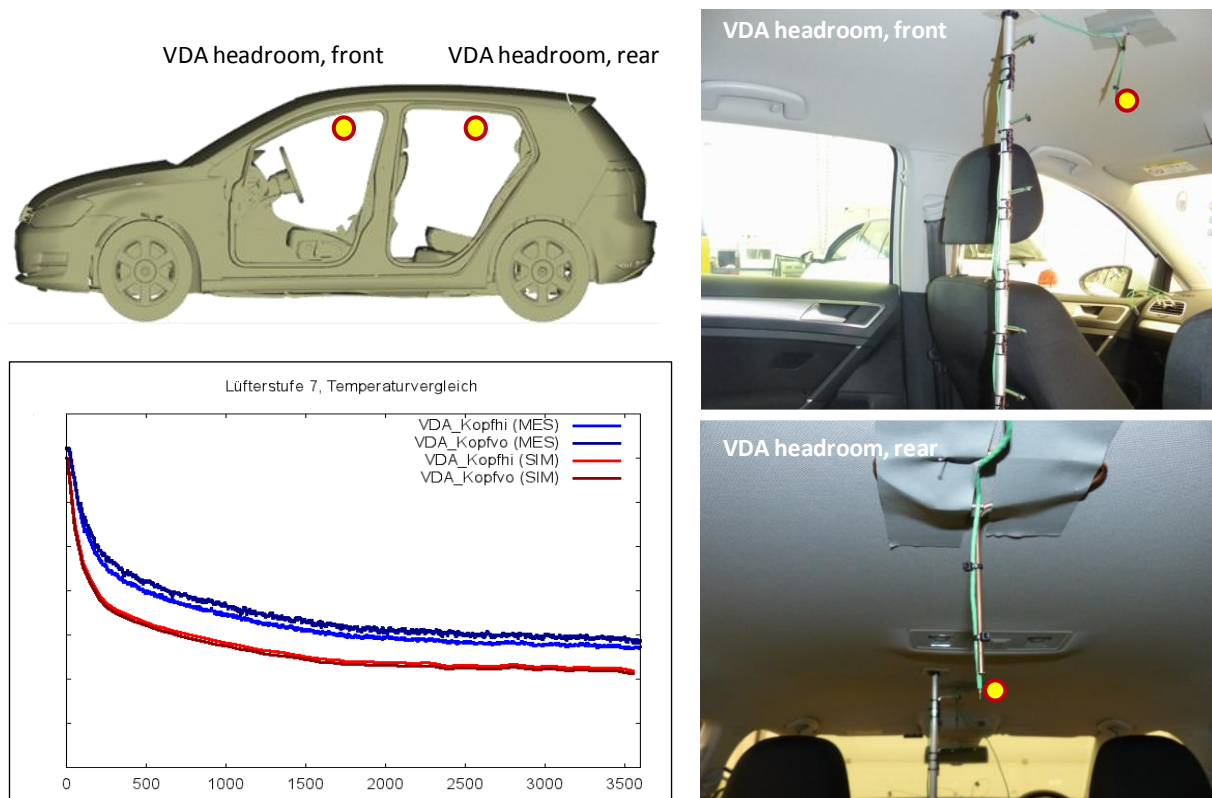


Figure 29: Test points in the headroom (center)

## 10. Conclusion

Within the framework of the BMBF-sponsored E-Komfort project, P+Z Engineering GmbH and Volkswagen AG worked together to enhance and validate methods for simulating thermal conditions in the vehicle cabin using THESEUS-FE software. The researchers used these methods for assessing novel climate control strategies in an e-Golf, investigating how a zonal climate control approach and the use of infrared emitters affect thermal comfort and energy consumption. Project team members undertook the following over the project's three-year lifespan: 1. Establishing and expanding simulation models that would model heat transfer mechanisms in as much detail as possible. This involved incorporating approaches such as thermal conductivity studies of the bonding technology used, CFD flow simulations, and sunlight simulation lamps from environmental chambers. 2. Developing simplified models that were then fine-tuned on the basis of detailed simulation models. 3. Performing large numbers of measurements in order to improve and/or validate the simulation models. In addition to increasing battery capacity in electric vehicles, important future concerns will include the demand for energy-saving options—especially in terms of climate control systems, which represent the second largest consumers of energy—so that e-vehicle range can be comparable to that of conventional vehicles. The simulation tools described here will

be important for conducting timely assessments of new ideas for saving energy in the vehicle development process. Simulation options—especially those for simulating global and local thermal comfort—will remain important in the automotive industry.

- [1] Fanger P. O.: “Thermal Comfort: Analysis and Application in Environmental Engineering.” Danish Tech. Press, Copenhagen, Denmark (1970)
- [2] Fiala D.: “Dynamic Simulation of Human Heat Transfer and Thermal Comfort.” PhD thesis, De Montfort University, Leicester (1998)
- [3] Beckmann, W.A. and Duffie, J.A.: “Solar Engineering of Thermal Processes.” 3rd edition, John Wiley & Sons, Inc., Hoboken, New Jersey (2006)
- [4] Zhang, H.: “Human Thermal Sensation and Comfort in Transient and Non-Uniform Thermal Environments.” PhD thesis, University of California, Berkley (2003)
- [5] DIN EN ISO 7730: “Analytische Bestimmung und Interpretation der thermischen Behaglichkeit durch Berechnung des PMV- und des PPDIndexes und der lokalen thermischen Behaglichkeit” [“Analytical determination and interpretation of thermal comfort using calculation of the PMV and PPD indices and local thermal comfort criteria”] (2003)
- [6] Lund C., Maister W., Lange C., Beyer B.: “Innovation durch Co-Simulation”, Wärmemanagement des Kraftfahrzeugs VI [“Innovation through Co-Simulation” in Vehicle Thermal Management VI], Expert Verlag (2008)
- [7] Schneider Th., Ellinger M., Paulke S., Wagner S., Pastohr, H. “Modernes Thermomanagement am Beispiel der Innenraumklimatisierung.” [“Vehicle Cabin Climate Control as an Example of Modern Thermomanagement.”] Automobiltechnische Zeitschrift (ATZ) 02, vol. 109, pp.162-169 (2007)
- [8] Lee C., Kwon J., Lee Y., Park J.: “Optimiertes Klimaanlage für erhöhte Reichweite von Elektrofahrzeugen.” [“Optimized Climate Control System for Improved Range of Electric Vehicles”] ATZ 06, vol. 114, pp. 486-491 (2012)
- [9] Wirth S., Eimler M., Niebling F.: “Thermische Isolation der Fahrgastzelle von Elektrofahrzeugen.” [“Thermal Insulation in the Passenger Compartment of Electric Vehicles”] ATZ 11, vol. 115, pp. 906-911 (2013)
- [10] Großmann H.: “Heizen, Lüften, Klimatisierung von PKW.” [“Vehicle Heating, Ventilation and Air Conditioning.”] Aerodynamik des Automobils, (ed. Hucho W.-H.), 5th edition, Vieweg Teubner Verlag

- [11] DIN EN ISO 14505-2: "Ergonomie der thermischen Umgebung – Beurteilung der thermischen Umgebung in Fahrzeugen –Teil 2: Bestimmung der Äquivalenttemperatur." ["Ergonomics of the thermal environment - Evaluation of thermal environments in vehicles - Part 2: Determination of equivalent temperature "] German version (2006)
- [12] Software THESEUS-FE: "Theory Manual." [www.theseus-fe.com](http://www.theseus-fe.com) (2014)
- [13] Incropera F.P., De Witt D.P.: "Fundamentals of Heat and Mass Transfer," 4th Edition (1996)
- [14] Paulke S., Wagner S., Schneider T.: "Some Considerations on Global and Local Thermal Comfort Based on Fiala's Thermal Manikin in THESEUS-FE." EUROSIM Ljubljana (2007)
- [15] DIN-EN-410: "Bestimmung der lichttechnischen u. strahlungsphysikalischen Kenngrößen von Verglasungen" ["Determination of luminous and solar characteristics of glazing"] (1998)
- [15] Gubalke, A., Thomschke, C. et al.: Körperbezogenes Klimatisierungskonzept für Kraftfahrzeuge [Vehicle climate control concept accounting for occupant bodies], Volkswagen Corporate Research, Stuttgart, Germany (2013)